Control of Extracellular Glutamate by Transporters in the CNS

by

Melissa A. Herman

A DISSERTATION

Presented to the Neuroscience Graduate Program

and the Oregon Health & Science University

in partial fulfillment of

the requirements for the degree of

Doctor of Philosophy

December 2009

School of Medicine
Oregon Health & Science University

CERTIFICATE OF APPROVAL

This is to certify that the Ph.D. dissertation of
MELISSA HERMAN
has been approved

Advisor, Craig Jahr

Member, Gary Westbrook

Member, Laurence Trussell

Member, John Williams

Member, Eric Gouaux

Table of Contents

Acknowledgements

There are many people to whom I am grateful for their support throughout the course of my dissertation. Above all, I thank my advisor, Craig Jahr, whose knowledge, patience, and creativity are unmatched. I am also grateful to the members of the Jahr Lab, my friends and colleagues, who have provided scientific guidance, life advice, and emotional support throughout the years. My friends and family have also been an integral part of this experience. I am so lucky to be surrounded by the amazing, interesting, brilliant people you are. Thank you for your support and perspective. Finally, I would like to thank my partner and best friend, Dan. His love and support have been invaluable throughout this process.

Abstract

Glutamate is the primary neurotransmitter governing excitatory synaptic transmission in the central nervous system. Because glutamate is not enzymatically degraded, after release from vesicles into the synaptic cleft or from other sources, it must be removed from the extracellular space. This task is accomplished by Na^+-dependent high-affinity glutamate transporters. Glutamate uptake by transporters prevents excitotoxicity and maintains the precision of synaptic transmission. In this thesis, I explored the role of transporters in controlling glutamate concentrations in and around synapses. In Chapter 1, we designed experiments to estimate the ambient concentration of glutamate in the extracellular space of rodent hippocampal brain slice. The value was ~25 nM, which is lower than the sensitivity of most glutamate receptors. Transporter function was necessary to maintain this low concentration of extracellular glutamate. We examined this finding in more detail in Chapter 2, exploring the distribution of ambient glutamate in the hippocampal neuropil. Extracellular glutamate is low throughout the neuropil indicating that transporters are not positioned to preferentially protect synaptic structures from ambient glutamate exposure. Instead, transporters prevent tonic activation of both synaptic and extrasynaptic receptors by maintaining low concentrations of ambient glutamate, likely due to the high density of transporters throughout the synapse-rich neuropil. These roles are integral in maintaining precise synaptic transmission.

Introduction

Excitatory synaptic transmission in the central nervous system (CNS) occurs when a glutamate-filled vesicle fuses with the plasma membrane of a presynaptic cell in a Ca^{2+}-dependent manner. The vesicle releases its contents into the synaptic junction, or cleft, activating glutamate receptors on the postsynaptic membrane. The glutamate then diffuses out of the cleft into the extracellular space. Unlike acetylcholine, the transmitter at the neuromuscular junction, glutamate is not degraded. Therefore, glutamate molecules in the extracellular space must be removed in order to prevent excitotoxicity and to prepare receptors for subsequent synaptic events (Vizi, 2000). This clearance of glutamate from the extracellular space is achieved by glutamate transporters.

In this thesis, I will argue that transporters control the glutamate concentration profile on a wide range of timescales—from submillisecond to seconds-and-greater. However, regardless of the time course of action, the over-arching role of the transporters is to ensure that synaptic transmission is precise and reliable.

Functional characteristics of glutamate transporters. The excitatory amino acid transporter (EAAT) family of proteins is responsible for clearing glutamate from the extracellular space of the CNS. Five EAATs (EAAT1-5) have been cloned (Storck et al., 1992; Pines et al., 1992; Kanai and Hediger, 1992; Fairman et al., 1995; Arriza et al., 1997). EAAT1 and 2 are predominantly expressed on the membrane of glial cells (Chaundry et al., 1995), whereas EAATs 3-5 are expressed on neurons (Rothstein et al., 1994; Dehnes et al., 1998). Studies in which glutamate transporters were removed

indicate that glial-expressed transporters are the dominant subtypes in maintaining glutamate below excitotoxic levels (Rothstein et al., 1996), but roles for the neuronal-expressed transporters have also been reported (Rothstein et al., 1994; Dehnes et al., 1998; Diamond, 2001; Brasnjo and Otis, 2001; Wadiche and Jahr, 2005).

Transporters accomplish glutamate uptake by harnessing the transmembrane electrochemical gradients of Na^+, K^+, and H^+. Co-transport of Na^+ and counter-transport of K^+ ions drive the process, though for many years the stoichiometry of this reaction was debated. Radiolabeling of Na^+ ions suggested that the stoichiometry was 2 Na^+ ions and one H^+ moving inward and one K^+ ion moving outward for every glutamate molecule (Kanai et al., 1995). However, using EAAT3 expressed in oocytes, Zerangue and Kavanaugh (1996) recorded the current associated with this electrogenic process and determined the dependence of the reversal potential on Na^+ and K^+ gradients. Using a zero flux equation (Equation 1), they calculated the reversal potential for the translocation process with different stiochiometries of ions at given concentrations. The observed reversal potential best matched a process with co-transport of 3 Na^+ ions and one H^+, and counter-transport of one K^+ ion per glutamate molecule. This is also the stoichiometry used by EAAT2 (Levy et al., 1998), and likely the other EAAT subtypes. The use of 3 Na^+ ions instead of 2 is crucial because it significantly boosts the thermodynamic driving force for glutamate translocation. Because each Na^+ ion uses the energy potential of the Na^+ concentration gradient, the $[Na_o]/[Na_i]$ term is raised to the power of the number of Na^+ in the stoichiometry (see Equation 1). Therefore, 3 Na^+ ions make the theoretical minimum extracellular glutamate concentration approximately 250

times lower than if only 2 Na^+ ions were involved (see review in Tzingounis and Wadiche, 2007).

Equation 1.

$$\Psi = (RT/F\ (n_{Na} + n_H - n_K - n_{Glu}))ln(([Na_o]/[Na_i])^{nNa}([Glu_o]/[Glu_i)^{nGlu}([H_o]/[H_i])^{nH}([K_i]/[K_o]))^{nK}$$

Where Ψ is the membrane potential, *R* is the gas constant, *T* is absolute temperature, *F* is Faraday's constant, *n* is the number of ions, *o* is the ion concentration outside the cell, and *i* is the ion concentration inside the cell.

In addition to the strong electrochemical driving force for glutamate translocation, the high expression density of transporters ensures efficient glutamate clearance. Using quantitative immunoblot techniques, Lehre and Danbolt (1998) determined that the glial transporter subtypes, EAAT1 and 2, are expressed on astroglial membrane at a combined density of ~10,800 μm^{-2} in the stratum radiatum of the adult rat hippocampus and ~5,400 μm^{-2} in the molecular layer of the cerebellum. In stratum radiatum, astrocytes tile the synapse-rich neuropil (Bushong et al., 2002; Bushong et al., 2004) with fine processes threading throughout the extracellular spaces (Ventura and Harris, 1999). Thus, the region is rich with transporter-laden membrane. Because of the large surface density of astroglial membrane in both stratum radiatum and the molecular layer of cerebellum, transporters are present at an effective concentration of 0.14-0.25 mM and 0.18-0.33 mM in the extracellular volume of each region, respectively (Lehre and Danbolt, 1998).

Theoretically, these characteristics of strong driving force and high expression density complement each other to make the glutamate transporters a powerful uptake system, but how is the efficiency of uptake monitored experimentally? Direct assays monitor uptake of substrate over time or currents associated with the transport cycle. Early studies of glutamate uptake efficiency used autoradiography to measure

translocation of titrated transporter substrates (Hertz, 1979; Blakely et al., 1988). Though this assay assesses the uptake capabilities of the transporters by monitoring labeled substrate, it cannot measure the rapid kinetics of the process or monitor the response to glutamate released under physiological circumstances. Fortunately, characteristics of the transporters allow for more sensitive reporting of the translocation process. As mentioned in a previous section, the stoichiometry of the glutamate translocation process is electrogenic, i.e. it results in 2 net positive charges with the movement of a glutamate molecule across the membrane. This electrogenic, or transport-coupled, current was first used to monitor glutamate transporter function (Brew and Attwell, 1987; Kanai et al, 1995; Wadiche et al., 1995a). However, because the transport process only results in 2 net positive charges per glutamate molecule, a detectable current requires a large number of activated transporters. In addition to the coupled transporter current, transporters exhibit a glutamate-sensitive anion conductance (Fairman et al., 1995). This anion current is activated by transport, but does not affect translocation (Wadiche and Kavanaugh, 1998), and is referred to as the “uncoupled” current. Because the anion conductance is channel-like, i.e. it is less dependent on temperature than the coupled conductance, this current is a more robust readout for transporter activity when recorded with a highly permeant anion in the intracellular compartment (Wadiche and Kavanaugh, 1998; Bergles et al., 2002). Both the coupled and uncoupled currents, however, have been detected in native cells in response to synaptic stimulation (Mennerick and Zorumski, 1994; Bergles and Jahr,1997, Diamond and Jahr, 1997, Otis et al., 1997; Diamond et al., 1998; Auger and Attwell, 2000; Brasnjo and Otis, 2004), and in both cases this is referred to as the synaptic transporter current (STC). In conjunction with kinetic transport cycle

models, the coupled STC has been used to predict the time course of glutamate in the extracellular space (Bergles and Jahr, 1997), though later work suggests this time course is complicated by the slow kinetics of the recorded STC (Diamond, 2005; Wadiche et al., 2006). Additionally, the uncoupled STC has been used to quantify the amount of glutamate transporters can clear (Otis et al., 1997). Therefore, electrophysiological recording of the STC, either coupled or uncoupled to transport, has been an invaluable tool for studying the function of transporters in response to synaptically-released glutamate.

Direct recordings of transporter currents demonstrate that they remove glutamate from the extracellular space. However, indirect assays have been most effective in identifying more subtle roles of glutamate uptake in synaptic transmission. The currents generated by iontropic glutamate receptors, such as the α-amino-3-hydroxyl-5-methyl-4-isoxazole-propionate (AMPA) or N-methyl-D-aspartic acid (NMDA) receptors, reflect concentration profiles of glutamate in the extracellular space, and are also the means by which synaptic communication occurs. Therefore, recording excitatory postsynaptic currents (EPSCs) with glutamate transport intact or inhibited will suggest whether transporters affect the glutamate concentration during physiological events. Characteristics such as transport cycle time, glutamate binding affinity, and location relative to the glutamate source may influence the role of glutamate transporters in different physiological situations requiring glutamate uptake. In the next three sections, I explore the role of transporters in governing glutamate concentrations over a range of time courses, and discuss how their intrinsic characteristics determine their impact on synaptic transmission.

The role of transporters on a seconds-and-greater time scale: maintenance of ambient glutamate. Neurotransmitters that are not degraded must be removed from the extracellular space by transporters (Curtis et al., 1960; Vizi, 2000). Ultimately, the ambient concentration of the transmitter left in the extracellular space reflects the homeostasis between the source and the uptake system. A tonic concentration of transmitters has been reported (Dunwiddie and Diao, 1994; Sah et al., 1989; Brickley et al., 2001). In many cases, ambient transmitters produce a standing current through tonic receptor activation (Dunwiddie and Diao, 1994; Sah et al., 1989; Brickley et al., 2001). For the inhibitory neurotransmitter, γ-aminobutyric acid (GABA), Santhakumar et al., (2006) used the standing current produced by iontotropic $GABA_A$ receptors in cerebellum to estimate the concentration of tonic GABA in the extracellular space. By comparing the amplitude of the standing current to the amplitude of currents produced by known concentrations of GABA applied to a cerebellar granule cell, they estimated an ambient GABA concentration of ~164 nM. This concentration is too low to affect most GABA receptors, except the high-affinity subtype of $GABA_A$ receptors expressed by granule cells (Santhakumar et al., 2006; Santhakumar et al., 2007). Tonic activation of the high-affinity glutamate receptor, the NMDA receptor, has also been reported (Sah et al., 1989; Cavelier et al., 2005; Cavelier and Attwell, 2005; Le Meur et al., 2007), though estimates of the ambient glutamate concentration have been controversial (for review, see Cavelier et al., 2005). A few key characteristics differ for GABA and glutamate transporters (for review, see Kanner, 2006). For instance, GABA transporters have a lower expression density (Chiu et al., 2002) and an ion stoichiometry of 2 Na^+ ions per GABA molecule

(Kavanaugh et al., 1992; Loo et al., 2000), making this system for transmitter uptake less efficient than glutamate transporters. However, the source of ambient GABA may also be different, making a weaker clearance mechanism adequate. Therefore, a direct translation of 164 nM ambient GABA to an ambient glutamate estimate is impossible.

Microdialysis studies estimate that ambient glutamate is 1-4 μM (Lerma et al., 1986; Baker et al., 2002; Nyitrai et al., 2006). Sah et al. (1989) substantiated this claim by reporting a large standing current recorded from NMDA receptors in CA1 neurons in hippocampal brain slices. The group reasoned that this large standing current was generated by a high concentration of ambient glutamate. This claim has recently come into question for a number of reasons. According to the activation and desensitization data for glutamate receptors, an ambient glutamate concentration of 1-4 μM would result in half-maximal activation of the high-affinity NMDA receptors (Patneau and Mayer, 1990; Featherstone and Shippy, 2008), low-dose desensitization of AMPA receptors (Trussell and Fischbach, 1989), and tonic activation of metabotropic glutamate receptors (mGluRs; Conn and Pin, 1997). This level of tonic activation would decrease sensitivity for detecting synaptic events and could lead to neuronal damage through excitotoxicity (Choi, 1992). However, the strong driving force and high expression density of glutamate transporters predicts a much lower tonic glutamate concentration. In fact, according to the thermodynamic calculations, the transporters are capable of reducing the extracellular glutamate concentration to the picomolar concentration range (Tzingounis and Wadiche, 2007). Because there is constant glutamate release, the actual concentration reached at the balance between uptake and release may be higher in the extracellular space of the brain. The ambient level of glutamate is at the equilibrium between uptake and the glutamate

source, because inhibiting glutamate transporters causes an increase in the extracellular glutamate concentration (Jabaudon et al., 1999). Therefore, even though ambient glutamate is higher than the theoretical minimum, transporters are working to maintain the extracellular concentration. Recent recordings of the standing current generated by ambient glutamate using modern brain slice preparation conditions and electrophysiological techniques (Cavelier et al., 2005; Cavelier and Attwell, 2005; Le Meur et al., 2007) reveal a smaller current than that reported by Sah et al.(1989). This could suggest the ambient glutamate concentration is lower. In consideration of this evidence, we re-examined the ambient glutamate concentration in hippocampal slice (Chapter 1).

Although the ambient glutamate concentration in the brain is likely much lower than 1-4 μM, functions for a tonic concentration in this range have been hypothesized. For example, in nucleus accumbens of the striatum, it has been suggested that the ambient glutamate concentration changes in response to withdrawal and resensitization of chronic cocaine-treated rats (Pierce et al., 1996; MacFarland et al., 2003; Moran et al., 2005). The tonic concentration, as assessed by microdiaylsis, dropped from ~6 μM to ~3 μM after withdrawal (Baker et al., 2003), thus presumably decreasing the activation of presynaptic inhibitory mGluRs and increasing synaptic activity (MacFarland et al., 2003; Moran et al., 2005). This increase in synaptic input could contribute to relapse behavior (reviewed by Kalivas, 2009). To reconcile the microdialysis reports, tonic presynaptic mGluR activation, and a small NMDA receptor-mediated standing current (Cavelier et al., 2005; Cavelier and Attwell, 2005; Le Meur et al., 2007), some have proposed that ambient glutamate is selectively high in extrasynaptic compartments and low in the

synapse (Pendyam et al., 2009; Kalivas, 2009). For this model to occur in the brain, transporters must preferentially protect the receptors on synaptic structures. Using a combination of electrophysiology and imaging, we address this hypothesis experimentally (Chapter 2).

The role of transporters on the millisecond time scale: limiting spillover between synapses. On the time scale of synaptic transmission, the glutamate concentration is much higher than the background, ambient level. In fact, it has been estimated that the glutamate transient concentration in the synaptic cleft following vesicle fusion can reach 1 mM (Clements et al., 1992; Diamond and Jahr, 1997). Recording of transporter currents clearly shows that glutamate spills out of the synaptic cleft, into the extrasynaptic environment, where it is removed by transporters on glial cells (Mennerick and Zorumski, 1994; Linden, 1997; Clark and Barbour, 1997; Bergles and Jahr, 1997). In a seminal study in the hippocampus by Bergles and Jahr (1997), the time course of the STC recorded in hippocampal astrocytes was compared to rapid agonist application-generated transporter currents recorded in outside-out patches. From this comparison, the group estimated the time course of the synaptically-released glutamate in the extracellular environment. They suggest that glutamate remains elevated in the extracellular space near astrocytic membranes for longer than 10 ms. In addition, optical measurements using a genetically encoded glutamate indicator suggest that synaptically-released glutamate remains elevated in the extracellular environment for hundreds of milliseconds, even in culture (Hires et al., 2008). On the other hand, a convincing study by Diamond (2005) suggests that transporters clear glutamate from the extracellular space much faster, with a

time constant of ~1 ms. This study claims that the STC time course is complicated by filtering of the recording and intrinsic kinetics of the transporters, therefore extrapolation of the extracellular glutamate time course from the STC is an overestimation.

To date, it is well accepted that receptor activation by glutamate spillover occurs in many brain regions (Diamond, 2002), and in many cases is limited under normal conditions by transporters (Barbour, 2001). Most studies have assessed this phenomenon by measuring changes in the kinetics of the AMPA or NMDA receptor EPSCs (for review see Tzingounis and Wadiche, 2007), the logic being that the EPSC decay, in part, reflects the duration of glutamate in the extracellular space and its access to extrasynaptic receptors. Therefore, if transporters determine the time course of glutamate in the extracelluar space, their inhibition will lengthen the EPSC decay. However, in the stratum radiatum region of hippocampus, early studies examining the decay kinetics of the AMPA receptor EPSC, reported no prolongation of the EPSC decay with inhibition of glutamate transporters (Hestrin et al., 1990; Sarantis et al., 1993; Isaacson and Nicoll, 1993). This result could be interpreted as a lack of spillover. It is possible that the densitization of AMPA receptors and the use of transportable substrate inhibitors of the transporters may have played a role in reaching this conclusion. In contrast, the NMDA receptor EPSC decay constant is increased with excess glutamate spillover and exacerbated by transporter inhibition (Arnth-Jensen et al., 2002). In the cerebellum, spillover at the parallel fiber to stellate cell synapse adds a slow component to the EPSC, which is enhanced by inhibition of glutamate transporters (Carter and Regehr, 2000). Additionally, in this region, knockout of EAAT1 indicates that this transporter subtype is responsible for preventing spillover to neighboring synapses at the climbing fiber to

Purkinje cell synapse (Takyasu et al., 2006). A recent study in retina suggests that spillover contributes to rentinal waves, which are thought to be important in visual development (Blankenship et al., 2009). This study also stressed the role of transporters in this process, as their pharmacological inhibition changed the timing of the retinal waves. Spillover to extrasynaptic NMDA receptors on spinal dorsal horn neurons also is limited by transporters (Nie and Wang, 2009).

It is less clear whether glutamate diffusing out of the synapse activates extrasynaptic receptors, neighboring synapse receptors, or both. At the hippocampal Schaffer collateral to CA1 synapse, the NMDA receptors that extend the EPSC decay with transporters blocked are different population from those activated by synaptic release with transport intact (Arnth-Jensen et al., 2002). Though this result suggests spill out of glutamate from the synapse, it does not distinguish between activation of extrasynaptic or neighboring synaptic receptors. Evidence in favor of spillover activating extrasynaptic receptors comes from the mossy fiber to CA3 pyramidal cell synapse of hippocampus, where transporter blockade enhanced activation of presynaptic mGluRs (Scanziani et al., 1997). Therefore, transporters regulate the activation of extrasynaptic receptors by limiting spill out of glutamate from the synapse. In the cerebellum, communication from climbing fibers to molecular layer interneurons occurs entirely through spillover (Szapiro and Barbour, 2007). This suggests that spillover may occur from specific synapses on one cell type to non-activated synapses on another. If the extent to which the synaptically-released glutamate can diffuse is limited by transporters, they play a crucial role in mediating communication between these neurons. More work must be done to examine whether glutamate released from one synapse can spill out and

activate receptors in an unstimulated neighbor synapse, and to what extent transporters play a role in limiting this process.

Is it possible that a specific population of transporters is responsible for limiting spillover? One intriguing idea is that neuronal transporters play a greater role in limiting spillover than glial transporter subtypes because of their perisynaptic location (Dehnes et al., 1998). It has been suggested that neuronal transporters are preferentially localized for preventing spill out of glutamate from the synapse (Amara and Fontana, 2002). Additionally, a number of studies have provided convincing physiological evidence for this role of neuronal transporters. In hippocampal CA1 neurons, transport activity of the neuronal transporter EAAT3 in CA1 neurons determines the extent of extrasynaptic NMDA receptor activation by spillover (Diamond, 2001). Also, in cerebellum extrasynaptic mGluR activation on a Purkinje neuron depends on the function of EAAT4 on that neuron (Brasnjo and Otis, 2001; Wadiche and Jahr, 2005). This result is particularly interesting because Bergmann glial cells, whose processes are closely associated with synapses onto Purkinje cells (Palay and Chan-Palay, 1974; Xu-Friedman et al., 2001; Spacek, 1985), express high levels of EAAT1. Therefore, it suggests that the transporters expressed on Purkinje cells must play the role of limiting the extent of extrasynaptic mGluR activation because of preferential location.

Regardless of whether transporters are expressed on neurons or astrocytes, it is clear they play a role in limiting the extent of glutamate spilling out from synapses. Whether glutamate spillover activates neighboring synapses is yet to be determined.

The role of transporters on the submillisecond time scale: Defining the time course of the synaptic glutamate transient. By far, the most controversial role for transporters has been that of synaptic glutamate clearance within the cleft. Originally, it was hypothesized that the time course of the synaptically-released transmitter in the cleft is determined by diffusion alone (Eccles and Jaeger, 1958). However, a study at the frog neuromuscular junction (NMJ) suggests a role for enzymatic degradation in clearing acetylcholine (Ach) released from a single quantum (Katz and Miledi, 1973). This study demonstrates that the time course of the Ach receptor-mediated miniature excitatory postsynaptic potential is prolonged, when degradation of Ach by acetylcholinesterase (AchE) was inhibited. An analogous role for glutamate transporters in determining the synaptic transient at central synapses has been much less clear.

Postsynaptic receptors are not saturated by glutamate released from a single quantum (Mainen et al., 1999; McAllister and Stephens, 2000; Oertner et al., 2002). Therefore, the kinetics of receptor activation in a miniature EPSC (mEPSC) should reflect the time course of glutamate in the synaptic cleft. In culture, pharmacological inhibition of glutamate transporters prolongs the decay of both NMDA receptor (Tong and Jahr, 1994) and AMPA receptor-mediated (Diamond and Jahr, 1997) mEPSCs. Diamond and Jahr (1997) simulated the time course of the glutamate transient to examine the role of glutamate transporters. The model predicts a glutamate transient with two components: a fast peak, and a slower tail. To simulate the slowing of the mEPSC decay, the transporters affect the tail of the glutamate transient, though still on the submillisecond time scale. Because the transport cycle itself is relatively slow (~10 to 70 ms, depending on the transporter subtype; Wadiche et al., 1995b; Bergles et al., 2002),

glutamate binding to a large number of transporters, rather than the actual uptake, must be responsible for the transporters' contribution to curtailing the synaptic transient (Tong and Jahr, 1994; Diamond and Jahr, 1997). In this buffered diffusion model, binding of glutamate by the transporters aids clearance by not allowing glutamate to diffuse back into the cleft (Franks et al., 2002).

Similar to the role of transporters in limiting spillover, the extent to which transporters define the time course of the synaptic glutamate transient may depend on their location relative to the release site. Though perisynaptic clustering of transporters has been reported (Zhou and Sutherland, 2004), how close to the synapse must transporters be to affect the quantal glutamate transient? At the NMJ, where transmitter degradation speeds Ach clearance, AchE is present within the synaptic cleft (Zacks and Blumberg, 1961). Although transporters could buffer the glutamate transient if they are located near the synapse rather than in the synapse (Franks et al., 2002); intrasynaptic localization would give transporters preferential, rapid access to cleft glutamate. Though immunhistochemical studies have found no evidence for intrasynaptic transporters, this may be due to epitope masking prohibiting binding of the antibody (reviewed by Fritschy, 2008). Additionally, a study examining transport of D-aspartate, an exogenous substrate of the transporters (Dowd et al., 1996), revealed uptake into the Schaffer collateral presynaptic terminal in stratum radiatum of hippocampus (Furness et al., 2008). This suggests, at certain synapses, a population of glutamate transporters may be positioned at the presynaptic terminal to shape the synaptic glutamate transient.

Transporter inhibition lengthens the time course of the synaptic glutamate transient at synapses in cultured neurons (Tong and Jahr, 1994; Diamond and Jahr, 1997).

However, a recent study in brain slices examining transporter inhibition on the decay of mEPSCs revealed no effect (Zheng et al., 2008), supporting the hypothesis that synaptic transient is cleared by diffusion alone (Eccles and Jaeger, 1958). Models generated to simulate these results suggest that transporters do not act on a time scale fast enough to contribute to clearance of the cleft glutamate transient (Zheng et al., 2008). However, there are a few caveats to this work. One problem is that transporter inhibition in slice increases the concentration of ambient glutamate in the extracellular space (Jabaudon et al.,1999; Cavelier and Attwell, 2005; Le Meur et al., 2007; Herman and Jahr, 2007), which could lead to desensitization of AMPA receptors. This would be less likely to occur in culture. Another problem is the diffusion coefficient used for the model simulations. It has been suggested that diffusion is more restricted in the slice than represented in the model (Nielsen et al., 2004), and an environment with a slower diffusion coefficient may rely more on transporters to aid in glutamate clearance.

Summary

Synaptic transmission occurs when a vesicle releases glutamate into the synaptic cleft and activates postsynaptic receptors. However, other factors affect the precision of this process on the individual synapse to network level. The goal of this dissertation was to investigate how transporters control extracellular glutamate, which could affect synaptic transmission.

First, we used electrophysiology and pharmacology to estimate the concentration of ambient glutamate in the extracellular space of hippocampal slice. We determined that this concentration is low, ~25 nM, and likely represents a state of balance between sources of glutamate and uptake by the transporters. Our interpretation of this result is

that the transporters compose a powerful glutamate clearance system that maintains extracellular glutamate at a concentration resulting in negligible tonic receptor activation.

Second, we examined the distribution of ambient glutamate in the extracellular compartments in hippocampal slice. The concentration estimate reached in the set of experiments described in Chapter 1 is a spatiotemporal average extracellular concentration. This estimate is derived from the current generated by all the tonically-activated NMDA receptors on the entire cell. Therefore, the possibility remained that receptors on non-synaptic structures were activated by a higher concentration of ambient glutamate, whereas receptors on synaptic structures were not activated, or protected from extracellular glutamate. This scenario is dependent on non-uniform expression of glutamate transporters, resulting in preferential protection of synaptic structures. We used electrophysiology and two-photon microscopy to resolve the location of NMDA receptors activated by ambient glutamate. We found that NMDA receptors on synaptic or non-synaptic structures were not tonically activated by extracellular glutamate, suggesting that transporters maintain a low ambient concentration throughout the neuropil.

Chapter 1.

Extracellular Glutamate Concentration in Hippocampal Slice

Melissa A. Herman and Craig E. Jahr
Vollum Institute, Oregon Health & Science University, Portland, OR USA

Corresponding Author: Craig E. Jahr
Vollum Institute
Oregon Heath & Science University
3181 SW Sam Jackson Park Road
Portland, OR 97239-3098, USA
jahr@ohsu.edu

Abstract:

Synaptic glutamate transients resulting from vesicular exocytosis are superimposed on a low baseline concentration of glutamate in the extracellular space. Reported values of baseline glutamate concentrations range up to 4 μM. If glutamate were present tonically at low micromolar concentrations, many receptors, especially the high affinity *N*-methyl-D-aspartate receptors (NMDARs), would be activated or desensitized, altering neuronal excitability. Using NMDARs expressed by CA1 pyramidal cells in acute hippocampal slices to monitor extracellular glutamate, we find that its baseline concentration is much lower, near 25 nM. In addition, superfusion of low micromolar concentrations of glutamate had no effect on neurons, indicating that glutamate transport prevents access to receptors within the slice. However, equipotent concentrations of NMDA, a non-transported agonist, depolarized neurons dramatically. We suggest that ambient concentrations of glutamate *in vivo* are also in the nanomolar range and are too low to cause significant receptor activation.

Introduction:

Glutamate transporters, along with diffusion, terminate excitatory neurotransmission mediated by exocytosis of glutamate-filled vesicles (Isaacson and Nicoll, 1993; Takahashi et al., 1996; Asztely et al., 1997; Diamond and Jahr, 1997; Wadiche and Jahr, 2005; reviewed by Danbolt, 2001). In addition, the densely expressed glutamate transporters maintain baseline levels of extracellular glutamate at concentrations low enough to prevent excitotoxicity (Choi, 1992; Rothstein et al., 1996;

Tanaka et al., 1997). Though the thermodynamic coupling of Na^+ and K^+ gradients to glutamate transport predicts a lower limit of 2 nM extracellular glutamate (Zerangue and Kavanaugh, 1996), the constant efflux of glutamate results in a higher steady-state ambient concentration in the extracellular space (Sah et al., 1989; Rossi and Slater, 1993; Lauri et al., 2006; Le Meur et al., 2007). Microdialysis studies report an *in vivo* ambient glutamate concentration as high as 1-4 μM (Lerma et al., 1986; Baker et al., 2002; Nyitrai et al., 2006). Given that the EC_{50} of the *N*-methyl-D-aspartate receptor (NMDAR) for glutamate is ~ 2 μM (Patneau and Mayer, 1990), this concentration range would have significant effects on neuronal excitability. In contrast to the microdialysis studies, measurements of ambient glutamate in acute brain slice suggest a much lower concentration (Cavelier et al., 2005; Cavelier and Attwell, 2005; Le Meur et al., 2007), although a definitive estimate is lacking, and whether one can extrapolate from brain slice to brain is unclear.

By measuring the tonic current mediated by NMDARs in CA1 pyramidal cells, we estimated the concentration of ambient glutamate. We determined that the tonic spatially and temporally averaged concentration of extracellular glutamate in acute hippocampal slices with intact glutamate transport is about 25 nM, 100-fold lower than previously reported (Lerma et al., 1986; Baker et al., 2002; Nyitrai et al., 2006). We suggest that this low concentration of extracellular glutamate is controlled by densely expressed glutamate transporters (Cavelier and Attwell, 2005; Danbolt, 2001; Garthwaite, 1985; Jabaudon et al., 1999).

Materials and Methods:

Slice preparation:

Postnatal day 15-19 rats (or mice) were deeply anesthetized with isofluorane and decapitated, as approved by the Oregon Health & Science University Institutional Animal Care and Use Committee. Hippocampi were removed and transverse slices (300 μm) were cut using a vibroslicer (Leica, Bannockburn, IL) in ice-cold solution containing the following (in mM): 110 choline chloride, 7 $MgCl_2$, 2.5 KCl, 1.25 KH_2PO_4, 0.5 $CaCl_2$, 25 $NaHCO_3$, 1.3 Na-ascorbate, 10 glucose (saturated with 95% O_2/ 5% CO_2). The slices were incubated for 30 to 45 minutes at 34°C then stored at room temperature in an external solution containing the following (in mM): 119 NaCl, 2.5 KCl, 2.0 $CaCl_2$, 1.3 $MgCl_2$, 1.0 NaH_2PO_4, 26.2 $NaHCO_3$, and 11 glucose (saturated with 95% O_2/ 5% CO_2).

Experimental procedures:

Whole-cell recordings were obtained, using an Axopatch-1B amplifier (Molecular Devices, Union City, CA), from CA1 pyramidal cells visually identified with differential interference contrast optics (Zeiss, Thornwood, NY). Slices were superfused with the above external solution with 2.5 mM $CaCl_2$, 100 μM picrotoxin, 10 μM NBQX, and 10 μM D-serine, except where noted. Experiments were performed at 32-35°C, with the temperature maintained by an in-line heating device (Warner Instruments, Hamden, CT), unless otherwise noted (see Figure 3). Patch pipettes (2.0-3.5 MΩ) were filled with an internal solution containing (in mM) 135 Cs^+ methanesulfonate, 8 NaCl, 10 HEPES, 10 Cs-BAPTA, 4 Mg-ATP, 0.4 Na-GTP, 0.2 verapamil (voltage-clamp experiments) or 135 K+ methanesulfonate, 8 NaCl, 10 HEPES, 10 K-BAPTA, 4 Mg-ATP, 0.4 Na-GTP

(current-clamp experiments). Slices from mouse were used for the cystine-glutamate exchange experiment only. Nucleated patch recordings were performed in the standard external solution with 5 mM $CaCl_2$ and 0 mM $MgCl_2$, using patch pipettes of ≤ 2.0 MΩ resistance. Electrophysiological recordings were acquired using custom software (J.S. Diamond, NINDS, Bethesda, MD) written in IgorPro (Wavemetrics, Lake Oswego, OR).

Agonists and antagonists were applied using a custom-built flow-pipe perfusion apparatus with a flow rate of ~ 0.1 ml/min positioned above the slice (Figure 1A). Flow-pipe solutions were continuously bubbled with 95% O_2/ 5% CO_2.

Data analysis and statistics:

AxoGraph X software (AxoGraph Scientific, Sydney, Australia) was used for analysis. Whole cell recordings were excluded from analysis if series resistance was ≥10 MΩ or changed ≥15% during the course of an experiment. Current amplitudes were measured at peak deflection relative to baseline. The current blocked by application of 100 μM D-(-)-2-amino-5-phosphonopentanoic acid (D-AP5; Tocris, Ellisville, MO) was normalized by the amplitude of the current evoked by 5 μM NMDA (Tocris) for cells recorded in the presence of TTX. Currents recorded from hippocampal astrocytes were normalized to the plateau of the test pulse, to scale for proportional rundown of the synaptic transporter current with increase in access resistance (Diamond et al., 1998). Statistical analysis was performed using Excel (Microsoft, Seattle, WA), and Instat (GraphPad software, San Diego, CA). Error bars on graphs correspond to the standard error of the mean (s.e.m.). Significance was determined using ANOVA (Dunett's or

Tukey's post hoc) or Student's *t* test. Non-linear regression analyses and EC_{50} estimates for dose-response data were performed with Prism (GraphPad software, San Diego, CA).

In every whole cell recording in which the standing NMDAR-mediated current was determined by block with D-AP5, the current evoked by 5 μM NMDA was also measured (see Results). To estimate the concentration of NMDA that would evoke a current the size of the standing current, each current evoked by 5 μM NMDA was set to 0.073, the fraction of the maximal response (1 mM NMDA) evoked by 5 μM NMDA in nucleated patches. The standing current was scaled by the factor required to scale the 5 μM NMDA current to 0.073. As the ratio of standing current to 5 μM NMDA current amplitude was 0.09, the standing current was 0.0065, i.e., less than 1% of the maximal current evoked by saturating NMDA. The concentration of NMDA necessary to evoke such a current was found by reading it off the abscissa of the dose-response curve at the point where the current was 0.65% of maximal.

Results:

Ambient glutamate generates a standing NMDAR current in hippocampus

Ambient extracellular glutamate activates an NMDAR-mediated current in hippocampal pyramidal cells (Sah et al., 1989; Cavelier and Attwell, 2005; Le Meur et al., 2007), which we used to estimate the concentration of glutamate in acute hippocampal slices. NMDAR currents were recorded in the presence of D-serine (10 μM), NBQX (10 μM), TTX (0.5 μM), and picrotoxin (100 μM) at +40 mV. To determine the amplitude of the standing NMDAR current, we applied the competitive NMDAR antagonist, D-AP5 (100 μM), via a flow-pipe to CA1 pyramidal neurons

(Figure 1A). D-AP5 application decreased the holding current by 73.7 ± 11.2 pA (Figure 1B; n = 7), blocking the NMDAR-mediated standing current generated by ambient glutamate. For comparison across cells, we divided this current amplitude by the current evoked by 5 μM NMDA (Figure 1B; 831 ± 74.5 pA; n = 7), a non-transported agonist (Garthwaite, 1985; Dowd et al., 1996). The resulting measure of the standing current was 0.090 ± 0.01 (n=7), a value that was used to quantify the ambient glutamate concentration. A similar ratio of standing current blocked by D-AP5 to current evoked by 5 μM NMDA, 0.14 ± 0.02 (n=8) was observed in medium spiny neurons of nucleus accumbens in the striatum (Supplementary Figure 1).

To confirm that the current evoked by 5 μM NMDA application was a direct effect of the agonist and not contaminated with depolarization-induced glutamate release from other cells in the slice, we recorded the action of 5 μM NMDA on CA1 pyramidal neurons in current-clamp in the same conditions. These cells were depolarized by 2.56 ± 0.9 mV during a 90 second application of 5 μM NMDA (n = 6). It seems unlikely that this depolarization would release enough glutamate to influence the evoked current.

It is possible that the ambient glutamate concentration is altered with changes in the level of synaptic activity. To test this, we investigated the magnitude of the NMDAR-mediated standing current while altering neuronal activity. The size of the current blocked by D-AP5 was not different in the presence or absence of TTX (Figure 1E; n = 7) nor with continuous 1 Hz stimulation of Schaffer collaterals, which evoked NMDAR excitatory postsynaptic potentials (EPSCs; Figure 1C-E; n = 7). This suggests that the concentration of ambient glutamate is unaltered by activity, which is consistent with the results of other groups that vesicular release of glutamate does not contribute to

the ambient extracellular concentration (Jabaudon et al., 1999; Cavelier and Attwell, 2005).

The ambient glutamate concentration is sub-micromolar

To estimate the average extracellular glutamate concentration, we first constructed dose-response relationships for NMDA and glutamate to which we could compare the normalized current blocked by D-AP5 (Figure 2). An accurate dose-response curve for glutamate could not be determined in the slice, because of the powerful uptake system present in the tissue (Garthwaite, 1985; Danbolt, 2001). Therefore, responses of pyramidal cells to the non-transported agonist NMDA (Dowd et al., 1996; 1-10 μM) were recorded in acute slices (Figure 2A; n = 6). These NMDA concentrations define only the foot of the dose-response curve (Patneau and Mayer, 1990). The entire dose-response curve could not be determined with whole-cell recordings, because the currents evoked with higher concentrations of NMDA were so large that we were concerned about the adequacy of the voltage-clamp. Therefore, the complete dose-response curves for both NMDA and glutamate were generated with nucleated patches from CA1 pyramidal cell somata (Figure 2B; n = 7). A semi-log plot was constructed, and the patch data were fitted with the Hill equation yielding an EC_{50} of 37.7 μM for NMDA and 1.8 μM for glutamate (Figure 2C), which are values close to those reported from dispersed neurons or neurons in primary culture at room temperature (Garthwaite, 1985; Patneau and Mayer, 1990). The whole-cell currents activated by 5 μM NMDA were scaled to the NMDA patch dose-response curve at the 5 μM point. The whole-cell measurements for 1-10 μM NMDA were well-described by the Hill equation

fit of the patch responses to NMDA (Figure 2C inset). When the whole cell data alone were fitted with the Hill equation, assuming a maximal response at 1 mM, the resulting fit was nearly identical (EC_{50} = 39 μM). From the Hill fit, a concentration of 0.790 ± 0.069 μM NMDA would be necessary to produce a current equivalent to the normalized D-AP5-blocked standing current (see Materials and Methods).

The concentration of glutamate required to activate a current of the same size as that blocked by D-AP5 was estimated by comparing the dose-response curves for NMDA and glutamate. Comparison of the EC_{50}s resulted in an NMDA to glutamate conversion factor of 0.048. Multiplying the NMDA dose-response regression fit by this conversion factor results in a good fit of glutamate responses (Figure 2C). Using this conversion factor, the ambient glutamate concentration necessary to produce the standing current in pyramidal cells is 37.9 ± 10.8 nM.

Agonists for the NMDAR can have different efficacies as well as different affinities (Lester and Jahr, 1992). With heterologously expressed NMDARs, the maximum response to glutamate is 1.2- to 1.5-fold larger than that of NMDA (Priestley et al., 1995). We tested this in our system by applying 100 μM glutamate and 1 mM NMDA, both saturating concentrations, to nucleated patches from CA1 pyramidal neurons. Glutamate produced a current that was 1.77 ± 0.08-fold larger than NMDA (Figure 2D, E; n = 5). Scaling the glutamate dose-response curve by this factor decreased our estimate of ambient glutamate to ~25 nM (Figure 2E).

Flow-pipe and bath applied drugs have comparable access to receptors

Flow-pipe drug applications are often used for patches and cultures, but not for acute brain slice. We performed control experiments to examine the extent to which drugs applied via flow-pipe penetrate the slice tissue and affect receptors on the recorded cell (Figures 1, 3). Flow-pipe application of 100 μM D-AP5 blocked the NMDAR-mediated EPSC by 94.4 ± 0.9% (87 ± 13% recovery with washout; Figure 1C, D; n = 8). In addition, we used the NMDAR-mediated current to investigate the concentration of agonist that reached the receptors (Figure 3). To do so, we compared the extent to which D-aminoadipic acid (DAA), a competitive low affinity NMDAR antagonist, would block currents evoked with bath or flow-pipe applications of 5 μM NMDA. If bath applied NMDA penetrated the slice better than flow-pipe applied NMDA, DAA should block the current evoked by bath application to a lesser extent. On the contrary, there was no difference in the block of currents evoked by flow-pipe and bath applied NMDA (69.4 ± 8.8% and 66.8 ± 8.7% of control, respectively; Figure 3A, B), suggesting that drug applied by flow-pipe reaches the receptors at a similar concentration as drug applied by bath.

Ambient glutamate estimate is not an artifact of washout

The ambient glutamate value of 25 nM could be an underestimate if endogenous extracellular glutamate were washed out of the slice with bath perfusion. We addressed this concern by comparing the magnitude of the standing NMDAR current blocked by 100 μM D-AP5 in control and while incubating the slice in 2 μM glutamate, a concentration in the range found by microdialysis (Lerma et al., 1986; Baker et al., 2002; Nyitrai et al., 2006). We found that the currents blocked by D-AP5 with 2 μM glutamate

in the bath were not different from controls (103.8 ± 7.21% of control; Figure 4A; n = 6). As we would expect a half-maximal activation of NMDARs with this glutamate concentration (equivalent to ~40 nM NMDA), and yet the standing current was not increased, we suggest that glutamate uptake is capable of maintaining extracellular glutamate at very low levels even in the presence of an endless supply of exogenous glutamate (Garthwaite, 1985). Another possible explanation for the low concentration of ambient glutamate we observed is that substrate for the source, cysteine for the cystine-glutamate exchanger (Baker et al., 2002), is being washed out of the slice. To test this, we recorded the NMDAR-mediated standing current in the presence of physiological concentrations of cysteine (0.3 to 3 μM) and saw no change from control conditions (Supplemental Figure 2). This suggests, in hippocampal slice, the cystine-glutamate exchanger is not the source for ambient glutamate.

If uptake is an important mechanism for maintaining low ambient glutamate levels, transporter antagonists should increase the standing current. As others have shown (Jabaudon et al., 1999; Baker et al., 2002; Cavelier and Attwell, 2005), application of the glutamate transporter competitive antagonist DL-threo-benzyloxyaspartic acid (TBOA; 200 μM; Figure 4B; n = 8), caused a rapid increase in current (τ_1 = 14.1 ± 2.85 sec; τ_2 = 65.3 ± 9.03 sec), but the current did not reach steady-state during a 2.5 min application suggesting a continual buildup of glutamate. The rising phase of this current reflects both the rate at which transporters are blocked as TBOA enters the slice and the rate at which glutamate is being released into the extracellular space. This current was mediated by NMDARs as it was blocked by D-AP5 (Figure 4C, D). Of the transporters expressed in the hippocampus, the astrocytic GLT-1 subtype accounts for ~80% of

uptake (Lehre and Danbolt, 1998; Danbolt, 2001). Blocking GLT-1 transporters with dihydrokainate (DHK; 100 µM; Fiacco et al., 2007) increased the standing current almost 4-fold, whereas blocking the remaining 20% of uptake with TBOA caused a further doubling of the current (Figure 4C, D). This suggests that the ambient glutamate concentration is controlled by transporters in a non-linear manner. In contrast, while DHK decreased the amplitude of transporter currents evoked in hippocampal astrocytes by Schaffer collateral stimulation, it did not decrease the amount of glutamate taken up, as measured by the integral of the transporter current (Figure 4E, F; see Diamond and Jahr, 2000). TBOA, on the other hand, blocked the transporter current leaving only the astrocytic response to elevated extracellular potassium (Figure 4E; Bergles and Jahr, 1997). These results suggest glutamate transporters play a dual role in the homeostasis of extracellular glutamate. First, they maintain low levels of ambient glutamate, and, second, they rapidly curtail the fast transients of glutamate following exocytotic release.

Diffusion of ambient glutamate from the surface of the slice into the bath inevitably occurs. However, given the sensitivity of extracellular glutamate concentration to transporter impairment and its resistance to change with exogenous glutamate in the bath, we suggest that tonic glutamate release and uptake are much more important in controlling the extracellular glutamate concentration in acute brain slice than diffusion into the bath.

NMDAR activation dramatically alters neuronal excitability

If extracellular glutamate were as high as previously reported (1-4 µM), what effect would this have on neuronal excitability? To determine this, we applied NMDA at

concentrations equivalent to this range of glutamate to cells recorded in current clamp in the absence of receptor antagonists. Using the conversion factor generated by the EC_{50}s of the NMDAR for glutamate and NMDA, 15, 30, and 60 μM NMDA should mimic effects of 0.75, 1.5, and 3 μM glutamate, respectively. All concentrations of NMDA produced profound depolarization and spiking (Figure 5). A 30 second application of 15 μM NMDA produced an average depolarization of 24.9 ± 10.1 mV, which was increased to 47.4 ± 22.9 mV with a 60 second application (Figure 5A, C). Application of 30 and 60 μM NMDA for 30 seconds produced more rapid and larger depolarizations (60.6 ± 6.60 and 60.9 ± 5.77 mV, respectively) accompanied by spike accommodation (Figure 5B, C). These results indicate that neurons in healthy acute slices are not normally enveloped by micromolar concentrations of glutamate. Were ambient glutamate to rise into the micromolar range, synaptic transmission, regenerative spiking, and neuronal health would be compromised. This also suggests that even *in vivo*, ambient glutamate levels must be in the nanomolar range.

Discussion:

Ambient glutamate is in the submicromolar range

To avoid excitotoxicity, glutamate transporters must maintain extracellular glutamate at a low concentration. However, previous studies report ambient glutamate concentrations of 1-4 μM *in vivo* (Lerma et al., 1986; Baker et al., 2002; Nyitrai et al., 2006). We propose that an ambient glutamate concentration in this range would not only have deleterious effects on neurons and synaptic transmission, but is also unrealistic given the efficacy of the glutamate uptake system. In the present study, we determined

that the ambient glutamate concentration in hippocampal brain slice is much lower than previously described. Our estimated value of 25 nM would have negligible actions on most glutamate receptors (Trussell and Fischbach, 1989; Patneau and Mayer, 1990; Conn and Pin, 1997), would not compromise neuronal excitability, and is in better agreement with the theoretical minimum concentration of glutamate transporters (2 nM; Zerangue and Kavanaugh, 1996; Levy et al., 1998). Additionally, because we observed a similar standing current to NMDA-evoked current ratio in medium spiny neurons of nucleus accumbens in striatum slice, we suggest that a similarly low concentration of ambient glutamate is present in the extracellular space of this region as well.

Were ambient glutamate in the micromolar range, NMDARs *in vivo* would be at half-maximum activation, because the EC_{50} of glutamate for the NMDAR is ~2 μM (Garthwaite, 1985; Patneau and Mayer, 1990). Additionally, because low micromolar concentrations of glutamate can also cause desensitization of AMPARs (Trussell and Fischbach, 1989), and may activate high affinity metabotropic glutamate receptors (Conn and Pin, 1997), synaptic transmission may be affected. We show that application of NMDA to acute brain slice at concentrations equivalent to 1-4 μM glutamate results in neuronal depolarization to nearly 0 mV and, as a consequence, complete spike accommodation. Because of these findings and considerations, we suggest that ambient glutamate levels *in vivo* are also in the nanomolar range.

Glutamate transport is highly efficient

The discrepancy in our estimate of the ambient glutamate concentration and that estimated by microdialysis may result from the exceedingly high concentration of

glutamate transporters expressed in the CNS (Danbolt, 2001). The significant volume of tissue damage surrounding the microdialysis probe (Clapp-Lilly, et al., 1999) could dramatically increase the distance between the probe tip and undamaged, transporter-expressing astrocytic membrane. We speculate that this transporter-free space surrounding the microdialysis probe, along with damage to the blood-brain barrier (Westergren et al., 1995), allows for build-up of extracellular glutamate and results in an artificially high ambient glutamate estimate. Our data support this speculation by showing that acutely blocking transport with TBOA increased the ambient glutamate concentration, even in conditions in which neuronal activity was blocked.

It is unlikely that the discrepancy between our results and previous *in vivo* studies result from 1) flow-pipe applied drugs not sufficiently blocking or activating NMDARs or 2) ambient glutamate washing out of the slice by diffusion into the bath. We addressed the first possibility by showing that flow-pipe applied D-AP5 reversibly blocked the NMDAR-mediated EPSC and that NMDA-evoked currents were not differentially blocked by the low-affinity antagonist DAA when NMDA was applied by flow-pipe or bath. We suggest that ambient glutamate in the slice is not lowered by diffusion into the bath, because the standing NMDAR-mediated current in the presence of 2 μM glutamate was not different from control and blocking transport with TBOA resulted in a rapid increase in standing NMDAR-mediated current indicating that glutamate release is relatively rapid. These results indicate that tonic release and uptake, rather than diffusion out of the slice, control the extracellular glutamate concentration. We suggest that, even *in vivo*, transporters have the capacity to keep extracellular glutamate at nanomolar concentrations. Ambient glutamate concentrations may not be

uniform throughout the CNS, or even in the same structures across development, as the expression levels of transporters can vary.

Two roles for glutamate transport: synaptic and non-synaptic uptake

As we and others (Cavelier and Attwell, 2005; Jaboudon et al., 1999) have shown, ambient levels of extracellular glutamate are not dependent on or altered by vesicular release, but rather require a different mechanism of efflux, possibly from glia (Cavelier and Attwell, 2005; Jabaudon et al., 1999; Le Meur, et al., 2007). Because synaptic release does not change ambient glutamate levels, the densely expressed transporters (Lehre et al., 1995; Lehre and Danbolt, 1998) must be capable of sequestering synaptically released glutamate very rapidly (Diamond, 2005; Wadiche et al., 2006) to prevent protracted diffusion. Thus, glutamate transporters appear to have distinct actions: rapid binding and uptake of vesicular release, which prevents or diminishes spillover, and a tonic clearance mode that maintains the average extracellular glutamate concentration at very low levels.

Figure 1: NMDAR-mediated currents in CA1 pyramidal cells

A, Schematic of flow-pipe configuration. Barrels were positioned at ~ 30˚ and ~1 mm from the recording pipette. **B,** Currents elicited from a CA1 pyramidal neuron by 5 μM NMDA and 100 μM D-AP5 (V_h = +40 mV). Bars indicate flow-pipe application of NMDA and D-AP5. Baseline currents have been offset. **C,** D-AP5 (100 μM) applied to CA1 pyramidal neuron during 1 Hz stimulation of Schaffer collaterals. **D,** Effect of D-AP5 on NMDAR EPSC amplitude. Bar indicates D-AP5 application. Inset: average traces from control, D-AP5 treatment, and washout (gray) periods. **E,** Average amplitude of NMDAR current with 1 Hz stimulation (n = 7), without stimulation or TTX (n = 14), or 0.5 μM TTX (control; n = 7).

Figure 1.

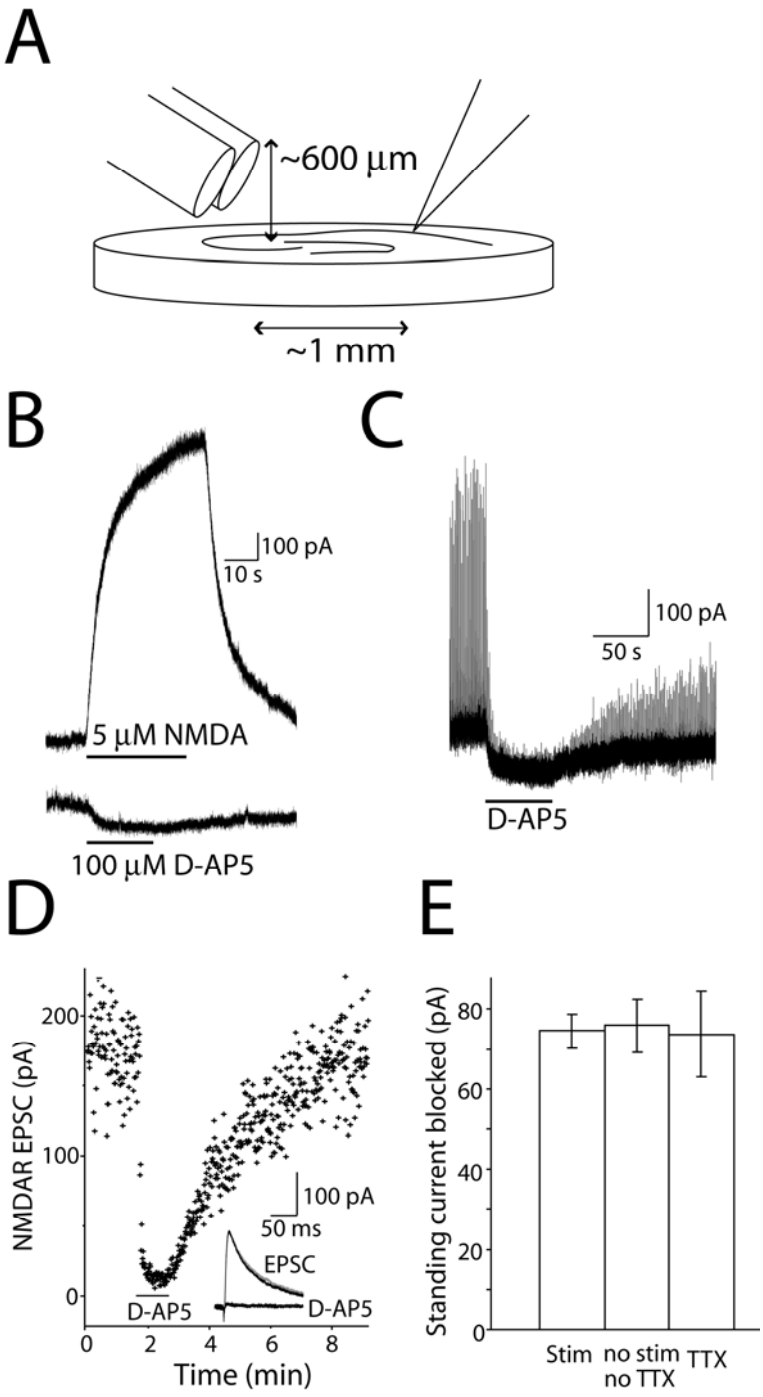
A
~600 µm
~1 mm
B
100 pA
10 s
5 µM NMDA
100 µM D-AP5
C
100 pA
50 s
D-AP5
D
NMDAR EPSC (pA)
200
100
0
100 pA
50 ms
EPSC
D-AP5
D-AP5
0
2
4
6
8
Time (min)
E
Standing current blocked (pA)
80
60
40
20
0
Stim
no stim
no TTX
TTX

Figure 2: Estimation of ambient glutamate concentration

A, NMDA evoked currents in a CA1 pyramidal neuron (V_h = +40 mV. Bar indicates applications of 1, 2, and 5 μM NMDA. Baseline currents have been zeroed. **B,** Nucleated patch currents produced by flow-pipe application of 5, 10, 20, 50, and 1000 μM NMDA (V_h = +40 mV). **C,** Semi-log plot of whole-cell (n = 6; gray circles) and nucleated patch (n = 6) current responses from application of NMDA (black squares) and glutamate (black circles; 0.5, 1, 3, 5, 100 μM; n = 6). Nucleated patch response were normalized to the maximum response. Whole-cell responses were scaled by the mean nucleated patch response to 5 μM NMDA. Line through NMDA responses is the non-linear regression fit with Hill equation of nucleated patch dose-responses (EC_{50} = 37.7 μM; n_H = 1.3). Line through glutamate responses is the NMDA fit shifted by EC_{50Glut}/ EC_{50NMDA}. Inset: Expansion of low concentration portion of NMDA dose-response curve. **D,** Nucleated patch responses to saturating concentrations of glutamate (100 μM) and NMDA (1 mM). **E,** Dose-response curves from (**C**) with glutamate-fit curve scaled by the efficacy ratio of 1.77. Arrows indicate the concentrations of glutamate and NMDA required to evoke currents of the same amplitude as that induced by ambient glutamate.

Figure 2.

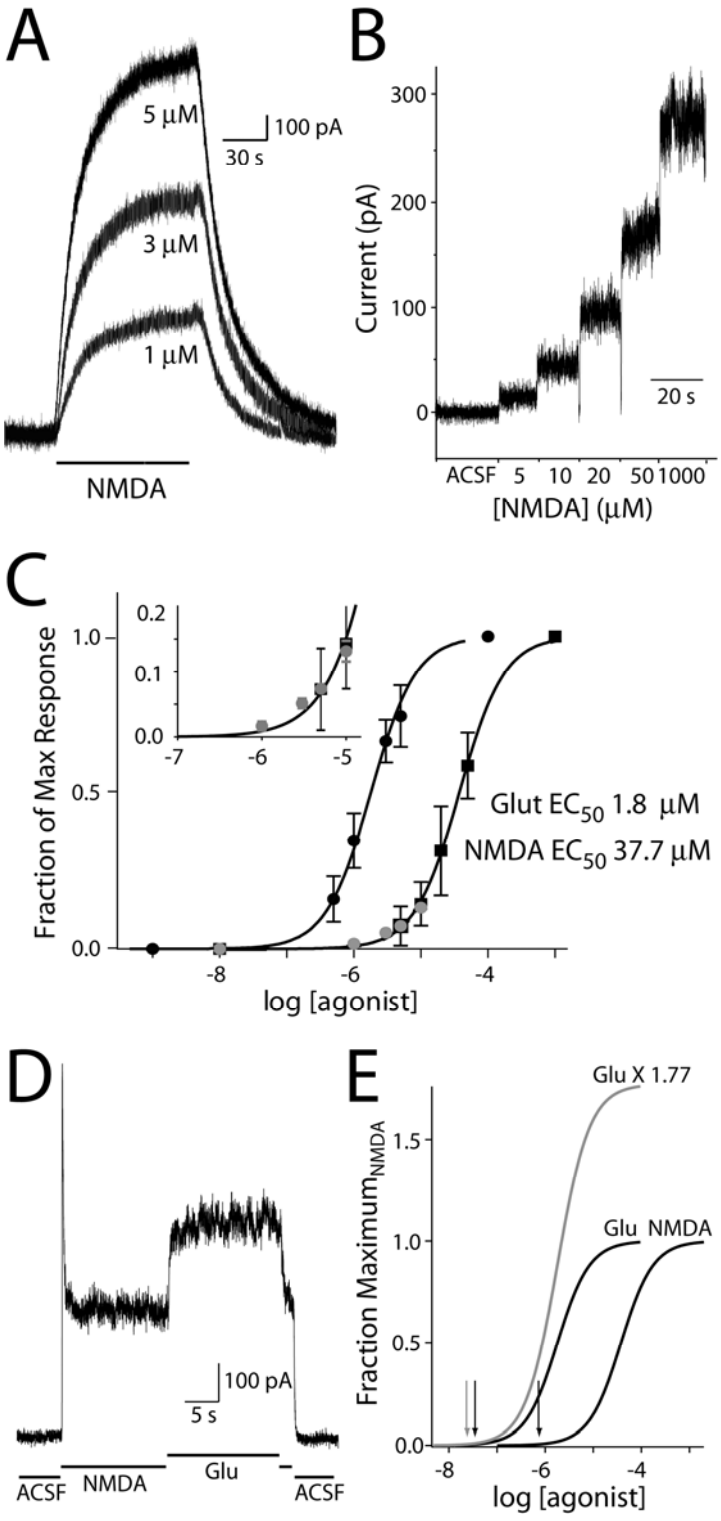
A
5 μM
3 μM
1 μM
100 pA
30 s
NMDA
B
Current (pA)
300
200
100
0
20 s
ACSF 5 10 20 50 1000
[NMDA] (μM)
C
Fraction of Max Response
1.0
0.5
0.0
0.2
0.1
0.0
-7 -6 -5
-8 -6 -4
log [agonist]
Glut EC50 1.8 μM
NMDA EC50 37.7 μM
D
100 pA
5 s
ACSF NMDA Glu ACSF
E
Glu X 1.77
Glu NMDA
Fraction Maximum NMDA
1.5
1.0
0.5
0.0
-8 -6 -4
log [agonist]

Figure 3: Solution exchange efficiency with flow-pipe applications

A, Currents evoked by 5 µM NMDA in control or in the presence of 70 µM DAA (V_h = +40mV; room temperature). Upper bars indicate bath and lower bars indicate flow-pipe applications. **B,** Flow-pipe or bath evoked currents blocked by DAA as a percentage of the control flow-pipe current (n = 4).

Figure 3.

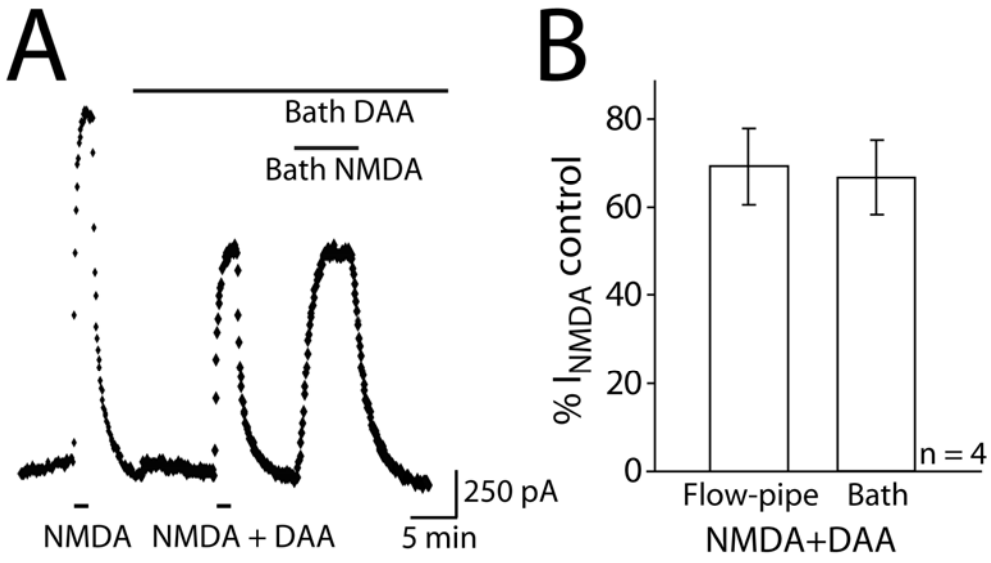

Figure 4: Glutamate transport maintains endogenous ambient glutamate

A, Standing current blocked by 100 μM D-AP5 in control (black) or with 2 μM glutamate (gray) in the bath. **B,** Current evoked by flow-pipe application of 200 μM TBOA. **C,** Standing currents blocked by 100 μM D-AP5 in control (gray), 100 μM DHK, or 100 μM TBOA in the bath. Baseline currents have been zeroed. **D,** Averaged amplitudes of currents in control, DHK, or TBOA normalized to the control current for each cell (n = 5). DHK and TBOA significantly increase the magnitude of the current blocked ($p < 0.05$ and $p < 0.01$, respectively). **E,** Schaffer collateral-evoked transporter current in a hippocampal astrocyte in control, 100 μM DHK, or 100 μM TBOA, in addition to 10 μM NBQX, 100 μM picrotoxin, and 50 μM D-AP5. All traces normalized to the plateau of the test pulse (see Materials and Methods). **F,** Average charge transfer of evoked transporter currents recorded in control and 100 μM DHK.

Figure 4.

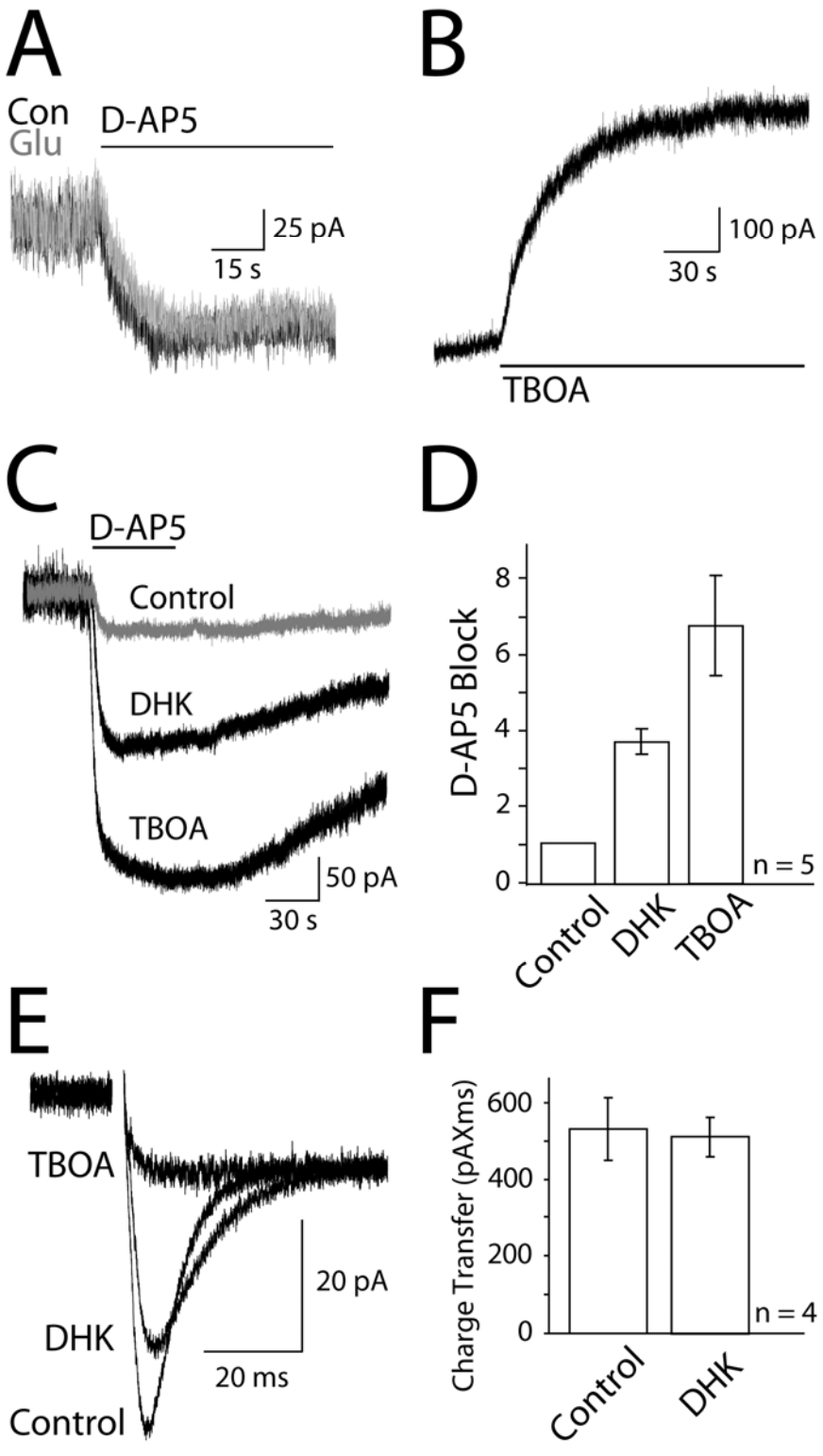
A
Con
Glu
D-AP5
25 pA
15 s
B
100 pA
30 s
TBOA
C
D-AP5
Control
DHK
TBOA
50 pA
30 s
D
D-AP5 Block
8
6
4
2
0
n = 5
Control
DHK
TBOA
E
TBOA
20 pA
DHK
20 ms
Control
F
Charge Transfer (pAXms)
600
400
200
0
n = 4
Control
DHK

Figure 5: NMDA application causes depolarization and spiking

A, Applications of 15 μM or (**B**) 30 μM NMDA to a CA1 pyramidal neuron in current clamp n (I = 0) in the absence of antagonists. Inset shows first spike burst on an expanded time scale indicated by asterisks (**A**). **C,** Average change in membrane potential with 30 (n = 6) or 60 (n = 5) second application of 15 μM NMDA, and 30 second applications of 30 μM (n = 6) or 60 μM NMDA (n =5).

Figure 5.

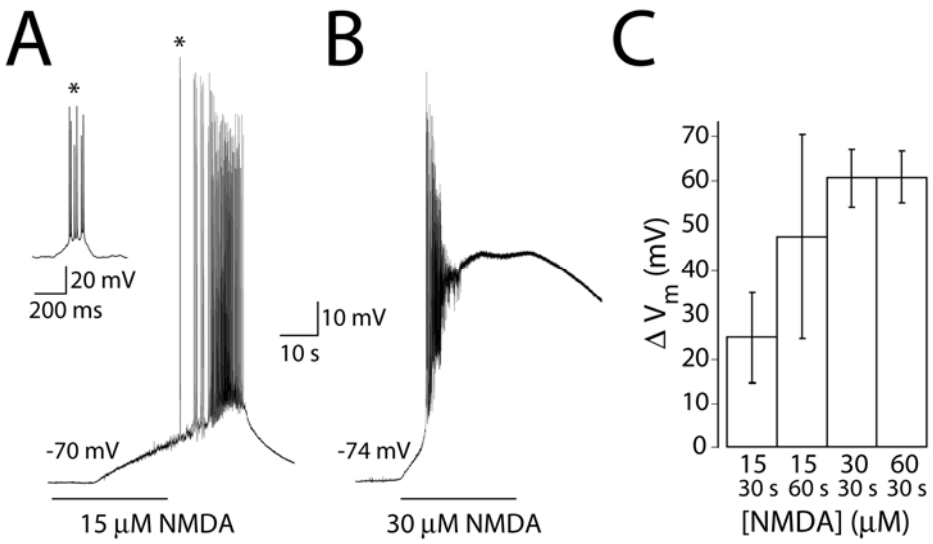

Supplementary Figure 1. NMDAR-mediated standing current in medium spiny neurons of striatal nucleus accumbens.

Currents elicited from a medium spiny neuron by 5 µM NMDA and 100 µM D-AP5 (V_h = +40 mV). Bars indicate flow-pipe application of NMDA and D-AP5. Baseline currents have been offset**.**

Supplementary Figure 1.

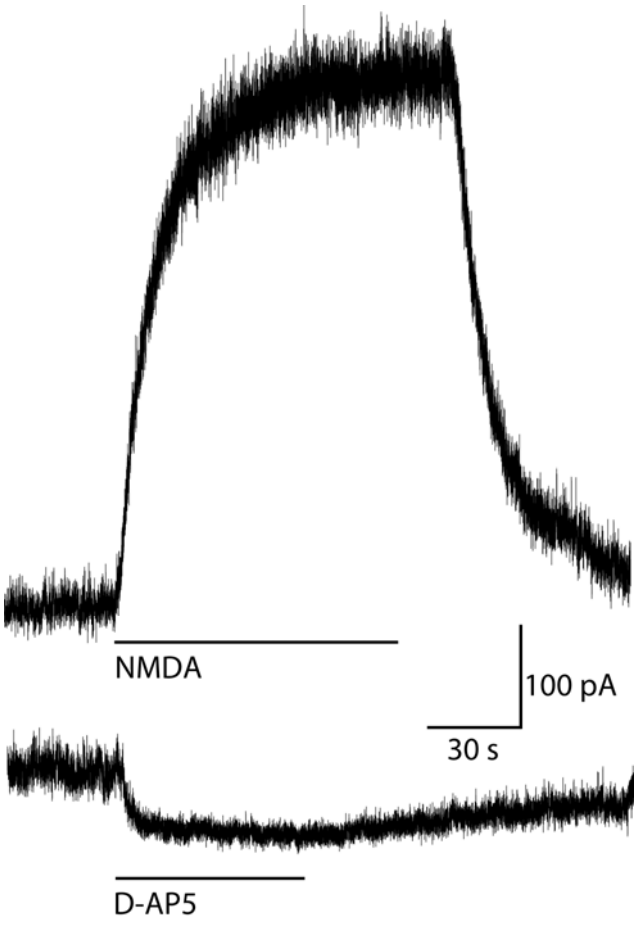

Supplementary Figure 2. Replacement of physiological cysteine concentrations does not alter the NMDAR-mediated standing current.

A, Standing current blocked by 100 μM D-AP5 in control (black) or with 0.3 μM cysteine (blue), and 3 μM cysteine (red) in the bath recorded from CA1 neuron in mouse hippocampal slice. **B**, Standing current blocked for each condition normalized to control and averaged between cells (n = 3).

Supplementary Figure 2.

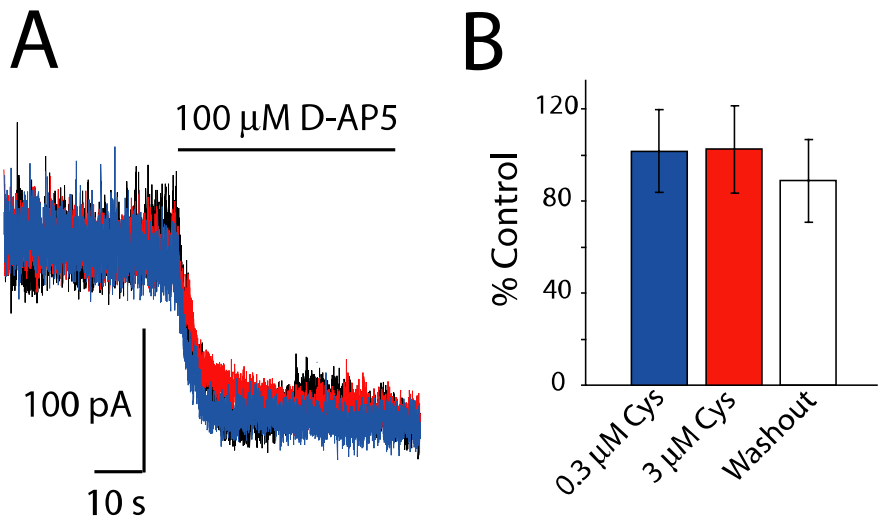

Chapter 2.

Distribution of extracellular glutamate in the neuropil of hippocampus

Melissa A. Herman and Craig E. Jahr

Vollum Institute, Oregon Health and Science University, Portland, OR, USA

Address for correspondence:
Craig E. Jahr
Vollum Institute
Oregon Health and Science University L474
3181 SW Sam Jackson Park Road
Portland, OR 97239

Phone: (503) 494-5471
e-mail: jahr@ohsu.edu

Abstract

Extracellular glutamate is maintained at a low ambient concentration, preventing excitotoxicity and preserving the sensitivity of receptors for detecting synaptic events. In a previous study, we estimated an ambient extracellular glutamate concentration of 25 nM surrounding hippocampal CA1 pyramidal cells based on the size of the tonic NMDA receptor-mediated current. Because this estimate was derived from whole cell recordings, the location of the receptors could not be resolved. As ambient glutamate levels may not be uniform throughout the neuropil, we used a combination of two photon laser scanning microscopy and electrophysiology, to compare tonic activation of NMDA receptors on synaptic and extrasynaptic structures. Synaptic NMDA receptors were not preferentially shielded from ambient glutamate, and there was not a steep concentration gradient of glutamate between extrasynaptic and synaptic extracellular compartments. We suggest that ambient glutamate is not compartmentalized in the extracellular space, but universally low throughout the neuropil of the hippocampus.

Introduction

Glutamate transporters maintain ambient concentrations of extracellular glutamate at low levels (Cavelier and Attwell, 2005; Cavelier et al., 2005; Le Meur et al., 2007; Herman and Jahr, 2007) and contribute to the termination of excitatory transmission by rapidly binding glutamate (Isaacson and Nicoll, 1993; Takahashi et al., 1996; Asztely et al., 1997; Diamond and Jahr, 1997; Wadiche and Jahr, 2005). Glutamate transporters can maintain low extracellular glutamate concentrations because of their high levels of expression, predominantly by astrocytes (Lehre et al., 1997; Lehre and Danbolt, 1998),

and the large driving force for translocation (Zerangue and Kavanaugh, 1996). The resulting low glutamate concentrations prevent tonic receptor activation and desensitization as well as excitotoxicity.

We have estimated that the spatiotemporal average concentration of extracellular glutamate in acute hippocampal slices is ~25 nM, a concentration that produces negligible tonic activation of glutamate receptors (Herman and Jahr, 2007). Our estimate was based on the amplitude of the tonic NMDA receptor (NMDAR)-mediated current recorded in CA1 pyramidal neurons. This current represents the activity of all NMDARs expressed by the neuron and would not detect any regional differences in activation, e.g., between synaptic and extrasynaptic receptors. Indeed, it has been suggested that ambient glutamate is not evenly distributed in the extracellular space and that a steep concentration gradient exists between synaptic and extrasynaptic compartments that results from a non-homogenous distribution of glutamate transporters (Pendyam et al., 2009). There is evidence that transporter expression is not uniform through the neuropil (Lehre and Danbolt, 1998; Lehre and Rusakov, 2002), which could allow for higher extrasynaptic glutamate concentrations. However, whether subpopulations of NMDARs are preferentially activated is not known.

We used two photon laser scanning microscopy (2PLSM) and electrophysiology to investigate whether extracellular glutamate is compartmentalized in acute slices of hippocampus. Pharmacological block of NMDARs had no effect on Ca^{2+} transients generated in dendritic shafts and spines of CA1 pyramidal neurons by depolarization, suggesting that ambient glutamate is too low to activate substantial numbers of NMDA receptors throughout the neuropil. Exogenous transportable and non-transportable

agonists of NMDARs could access both synaptic and extra-synaptic receptors, suggesting there is no preferential protection of spines by glutamate transporters. Finally, block of glutamate transporters did not flood the synapse with glutamate.

Results

Neuronal depolarization decreases Mg^{2+} block of NMDAR channels and increases their Ca^{2+} flux. Activation of NMDARs with glutamate uncaging can boost the Ca^{2+} generated by back-propagating action potential (bAP; Carter and Sabatini, 2004). Using 2PLSM, we measured Ca^{2+} transients in the dendrites of CA1 pyramidal neurons in acute hippocampal slices in response to depolarizations to determine if there is a higher concentration of ambient glutamate at extrasynaptic NMDARs (dendritic shafts) than at synaptic NMDARs (spines). Pyramidal neurons were recorded in current clamp and filled through the pipette with the Ca^{2+} indicator, Fluo-5F (300 µM), and the morphological dye, Alexa Fluor 594 (15 µM). We compared Ca^{2+} transients evoked by a single bAP in dendritic shafts and spines in control conditions (10 µM D-serine; 10 µM NBQX; 100 µM picrotoxin) and with NMDA receptors blocked by D-AP5 (10 µM; Figure 1). Though bAPs evoked Ca^{2+} transients in both dendritic shafts and spines (Figure 1B, black traces), D-AP5 did not alter the transients in either structure (Figure 1B, gray traces; dendrite 105 ± 5.5% of control, spine 109 ± 5.8% of control; n = 11). This result suggests that there is little tonic activation of NMDARs in either dendritic shafts or spines by ambient levels of glutamate.

This experiment is not ideal for detecting activation of a small number of NMDARs. The brief depolarization of the bAP is too short to engage the slow component

of NMDAR Mg^{2+} unblock (Kampa et al., 2004). In addition, the increase in Ca^{2+} influx through NMDARs during a bAP may be very small relative to the Ca^{2+} transient resulting from voltage-gated calcium channels (VGCCs). To increase the signal-to-noise of our recordings, we examined the affect of D-AP5 on Ca^{2+} transients generated by 40 ms voltage steps in the presence of tetrodotoxin (TTX; 0.5 µM) and mibefradil and nimodipine (20 µM for each), antagonists of the predominant VGCCs on dendrite shafts and spines of CA1 pyramidal cells (Bloodgood and Sabatini, 2007). Mibefradil and nimodipine greatly decreased the Ca^{2+} transient generated by a 40 ms voltage-step to +5 mV in dendrite (79 ± 2.8% decrease; $n = 5$; $P < 0.01$) and spine (75 ± 4.5% decrease; $n = 5$; $P < 0.01$).

To test whether NMDARs contribute to the Ca^{2+} signal in the presence of VGCCs antagonists, we measured the effect of D-AP5 in dendritic shafts and spines of apical dendrites (Figure 2A). D-AP5 did not reduce the Ca^{2+} signal in either structure, again suggesting that ambient glutamate concentrations are very low in both compartments. To test whether our method could detect NMDAR activation, we repeated the experiment in the presence of bath applied NMDA, a non-transportable agonist. NMDA (5µM, equivalent to ~250 nM glutamate; Patneau and Mayer, 1990; Herman and Jahr, 2007), produced a significant voltage step-evoked Ca^{2+} transient in both structures (dendrite, 2.46 fold increase on average, $P < 0.01$; spine, 7.54 fold increase on average, $P < 0.001$; Figure 2). These results indicate that this method has the sensitivity to detect NMDAR activation and that ambient glutamate is low in both compartments. The degree of compartmentalization of ambient levels of glutamate did not differ across regions of neuropil, because recordings from apical dendrities (stratum radiatum) and basal

dendrites (stratum lucidum) were not different. Therefore, data from both regions were pooled (Figure 2B).

Our results suggest that baseline ambient levels are universally low in the neuropil. However, our experiments rely on the expression of extrasynaptic NMDARs to report glutamate levels. If expression is low (Sobczyk et al., 2005), extrasynaptic glutamate levels could be higher than those in the synapse if transporters preferentially protect synaptic NMDARs from ambient glutamate. Although we show significant activation of receptors to bath applied NMDA, the Ca^{2+} transients observed in dendritic shafts could result from diffusion of bound indicator from the numerous surrounding spines. We tested these caveats in two ways. To test for higher expression levels of transporters surrounding synaptic receptors, the transporter substrate and NMDAR agonist, L-aspartate, was focally applied to pyramidal cell apical dendrites from an iontophoresis pipette while recording Ca^{2+} transients during voltage steps as above. Iontophoresis of L-aspartate, evoked Ca^{2+} transients in both dendritic shafts and spines (Figure 3, black traces). These Ca^{2+} transients were generated by L-aspartate activation of NMDARs because they were greatly reduced without L-aspartate ejection (to 23.7 ± 6.7% in shafts, $P < 0.001$ and 11.2 ± 3.8% in spines; $n = 5$; $P < 0.001$; Figure 3, red traces), and recovered when L-aspartate ejection resumed (125.8 ± 24.6% of the first L-aspartate response in shafts and 73.3 ± 7.7% in spines; $n = 5$; Figure 3, gray traces). That dendritic shafts and spines responded similarly to L-aspartate suggests that spine NMDARs are not preferentially protected by transporters. However, iontophoretic L-aspartate potentially could overwhelm the uptake system, negating the expected effects of differential expression levels. To test for this possibility, Ca^{2+} transients were recorded

during the ejection of L-aspartate in the presence of the transporter antagonist, TBOA (100 μM). This resulted in an increase in L-aspartate -evoked Ca^{2+} signal in both shafts and spines (237 ± 37%, $P < 0.001$ and 182 ± 30%; $n = 5$; $P < 0.05$, respectively; Figure 3, blue traces), suggesting that focally-applied L-aspartate does not overwhelm transporters.

Finally, if very few NMDARs are expressed extrasynaptically and ambient glutamate in synapses is maintained at much lower concentrations because of a protective barrier of transporters (Pendyam et al., 2009), blocking transporters should flood synapses with extrasynaptic levels of glutamate and result in large Ca^{2+} transients in spines. However, in the absence of L-aspartate ejection, TBOA (100 μM) did not alter Ca^{2+} levels in either shafts or spines (Figure 3, green traces). This result also indicates that the increase in Ca^{2+} levels produced by TBOA in the presence of L-aspartate does not result from an independent action of TBOA.

Discussion

The concentration of glutamate in the extracellular space is, on average, maintained at very low concentrations, sufficient only for activating exceedingly few high affinity NMDA receptors (Cavelier and Attwell, 2005; Herman and Jahr, 2007; Jabaudon et al., 1999; Le Meur et al., 2007). These prior studies did not address whether glutamate concentrations vary across extracellular compartments. Although prior reports suggested that, as a result of differential distribution of glutamate transporters, ambient glutamate levels may be maintained at much lower levels in the synaptic cleft than in extrasynaptic regions (Pendyam et al., 2009). We find no evidence for such compartmentalization. First, glutamate levels were not high enough to activate significant

numbers of extrasynaptic NMDA receptors and, second, synaptic NMDA receptors were not preferentially protected by glutamate transporters.

We observed NMDA receptor-mediated Ca^{2+} elevations in dendrites only in response to applications of exogenous NMDA or L-aspartate suggesting that extrasynaptic receptors are rarely bound by ambient levels of glutamate. However, whether there are enough extrasynaptic NMDA receptors on dendrites to detect ambient levels is unclear (Sobcyzk et al., 2005). The dendritic Ca^{2+} transients evoked by exogenous NMDA and L-aspartate may have resulted from the diffusion of bound indicator from neighboring dendritic spines, i.e., from Ca^{2+} flux through synaptic NMDA receptors. However, extrasynaptic concentrations cannot be very high because transporter inhibition does not flood the synaptic cleft with glutamate. In addition, the synaptic compartment cannot be overly protected from ambient glutamate by a defensive perimeter of transporters because applying the transportable NMDA receptor agonist, L-aspartate, readily activates synaptic receptors. Even though the small percentage of extant NMDA receptors activated by ambient glutamate is increased by transporter antagonists (Jabaudon et al., 1999; Cavelier et al., 2005; Le Meur et al., 2007; Herman and Jahr, 2007), the likelihood of observing NMDA receptor-mediated Ca^{2+} influx at the single spine level is apparently vanishingly low, despite the sensitivity of 2PLSM to detect single NMDA channel openings (Christie and Jahr, 2007; 2009; Nimchinsky et al., 2005).

Can our results be reconciled with studies suggesting a non-homogenous distribution of glutamate transporters in the extracellular space? Immuno-EM studies report that astrocytes express a higher density of glutamate transporters on membranes facing the synapse-rich neuropil than on membranes facing non-synaptic dendrite or

astrocyte processes (Lehre and Danbolt, 1998). In stratum radiatum, the density only decreases two-fold, from ~10,000 to ~5,000 per μm^2 of astrocyte membrane. Using this distribution of transporters, models of the extracellular space predict that theglutamate concentration is in the range of 30-50 nM throughout the neuropil of hippocampus (Zheng et al., 2008), similar to previous experimental estimates (Cavelier and Attwell, 2005; Herman and Jahr, 2007). In addition, EM studies indicate that transporter-laden astrocytic processes thread throughout the neuropil of hippocampal stratum radiatum, associating both with putative synaptic and non-synaptic CA1 pyramidal structures (Ventura and Harris, 1999; Witcher et al., 2007). Together with our present findings, these studies indicate that glutamate transporters are present throughout the neuropil and keep extracellular glutamate levels universally low.

Future direction: Our results suggest that there is no significant compartmentalization of extracellular glutamate in the neuropil of hippocampus. However, the Ca^{2+} imagining experiments are in part limited by the density of extrasynaptic NMDARs, which is lower than that at synapses (Sobcyzk et al., 2005). An additional experiment may resolve this issue. In this experiment, we will compare the extent of desensitization of synaptic and extrasynaptic AMPARs. Extrasynaptic AMPARs are expressed at densities high enough to observe currents with electrophysiological recordings (Matsuzaki et al., 2004). If extrasynaptic glutamate levels are high relative to those in the synaptic cleft, extrasynaptic receptors should be desensitized to a greater extent. To compare the level of desensitization, I will use two-photon uncaging of glutamate to generate focal AMPAR responses from a spine and neighboring dendrite. The uncaging will be repeated after

desensitization is inhibited with cyclothiazide (CTZ). If extrasynaptic glutamate is at a higher concentration than in the cleft, the ratio of AMPAR responses (control/CTZ) will be lower in dendrites than in spines. We expect that the ratio of the responses in both structures will be the same.

Experimental Procedures

Slice preparation and electrophysiology

Sprague-Dawley rats (P15-21) were deeply anesthetized with isofluorane and decapitated in compliance with the Oregon Health & Science University Institutional Animal Care and Use Committee approved protocol. Hippocampi were dissected out, and transverse slices were cut (300 μm) on a vibroslicer (Leica) in an ice-cold solution containing (in mM): 110 choline chloride, 7 MgCl2, 2.5 KCl, 1.25 sodium phosphate monobasic, 0.5 CaCl2, 1.3 Na-ascorbate, 25 NaHCO3, and 10 glucose (saturated with 95% O_2/ 5% CO_2). Slices were transferred to an incubation chamber containing the following extracellular solution (ECS, in mM): 119 NaCl, 2.5 KCl, 2.0 $CaCl_2$, 1.3 $MgCl_2$, 1.0 NaH_2PO_4, 26.2 $NaHCO_3$, and 11 glucose (saturated with 95% O_2/ 5% CO_2). Slices were incubated at 34 C for 30-45 min then maintained at room temperature.

Whole cell recordings were obtained from CA1 pyramidal neurons visually identified by location with infared contrast optics (Dodt). The intracellular solution (ICS) used for current clamp experiments contained (in mM) 135 K MeSO3, 10 HEPES, 4 MgCl2, 4 Na2ATP, 0.4 Na3GTP, and 10 phosphocreatine. The ICS for voltage clamp experiments contained (in mM) 125 CsMeSO3, 20 HEPES, 4 MgCl2, 4 Mg2ATP, 0.4 Na3GTP. To each ICS, 15 μM Alexa 594 and 300 μM Fluo-5F (Invitrogen, Carlsbad,

CA) was added on the day of recording for imaging purposes. Recordings for both clamp modes were made using pipettes with resistance of 2-4 MΩ with either an Axopatch 1-D (Axon Instruments, Union City, CA) or a Multiclamp 700B (Molecular Devices, Union City, CA) amplifier. Electrophysiological data were collected using either Axograph X (Axograph Scientific, Sydney, Aus) or custom software (J.S. Diamond, NINDS, Bethesda, MD) written in IgorPro (Wavemetrics, Lake Oswego, OR).

During recordings, slices were superfused with the incubation ECS described above, temperature elevated to 32-34ºC using an in-line heater (Warner Instruments), with the addition of pharmacological agents purchased from Tocris (tetrodotoxin, NMDA, D-serine, TBOA), Ascent Scientific (NBQX, D-AP5), and Sigma Aldrich (picrotoxin, mibefradil, nimodipine) in specific combinations according to experimental design (see **Results and Discussion**). In voltage clamp experiments where VGCC signal was reduced, a rundown protocol (60-120 trials of 40 ms 70 mV voltage-steps) was preformed in the presence of VGCC antagonists prior to imaging.

Iontophoresis pipette contained 100 μM Asp. Asp was ejected by leak or small negative holding current (< -200 pA), and ejection was stopped by applying positive backing current (1-2 nA).

Two-photon imaging

Green and red fluorescence were simultaneously monitored using a purpose-built two-photon laser scanning microscope (as described by Christie and Jahr, 2008). Images were collected and line scans were performed (32 lines at 2 ms/line) using Scan Image software (Pologruto et al., 2003). Change in fluorescence over time in line scans was

quantified by dividing baseline-subtracted green channel traces by the paired trace collected in the red channel (Δ G/R, Sabatini et al., 2002).

Data Analysis

Data analysis was performed using Image J, Microsoft Excel, Axograph X, and BrightStat. Student's t test and ANOVA (Friedman with Conover post hoc) were used when appropriate. For voltage-step experiments, cells were rejected if the average amplitude of the washout response was significantly smaller than control as determined by statistical analysis of points in the 50-60 ms range of line scan image. P values > 0.05 were considered significant.

Figure 1. D-AP5 has no effect on bAP-evoked Ca^{2+} signal in dendrite or spine.

(**A**) *Top Left* 2PLSM image of dendrite and spine from a CA1 pyramidal neuron. *Bottom Left* Green channel fluorescence transient in line-scan mode in response to a bAP (indicated by arrow). Image is an average of several trials. *Right* Average AP evoked by current injection at soma.(**B**) Average increase in fluorescence with a bAP measured from line-scan image of dendrite (*left*) and spine (*right*) in control (black traces) and in the presence of 10 µM D-AP5 (gray traces).

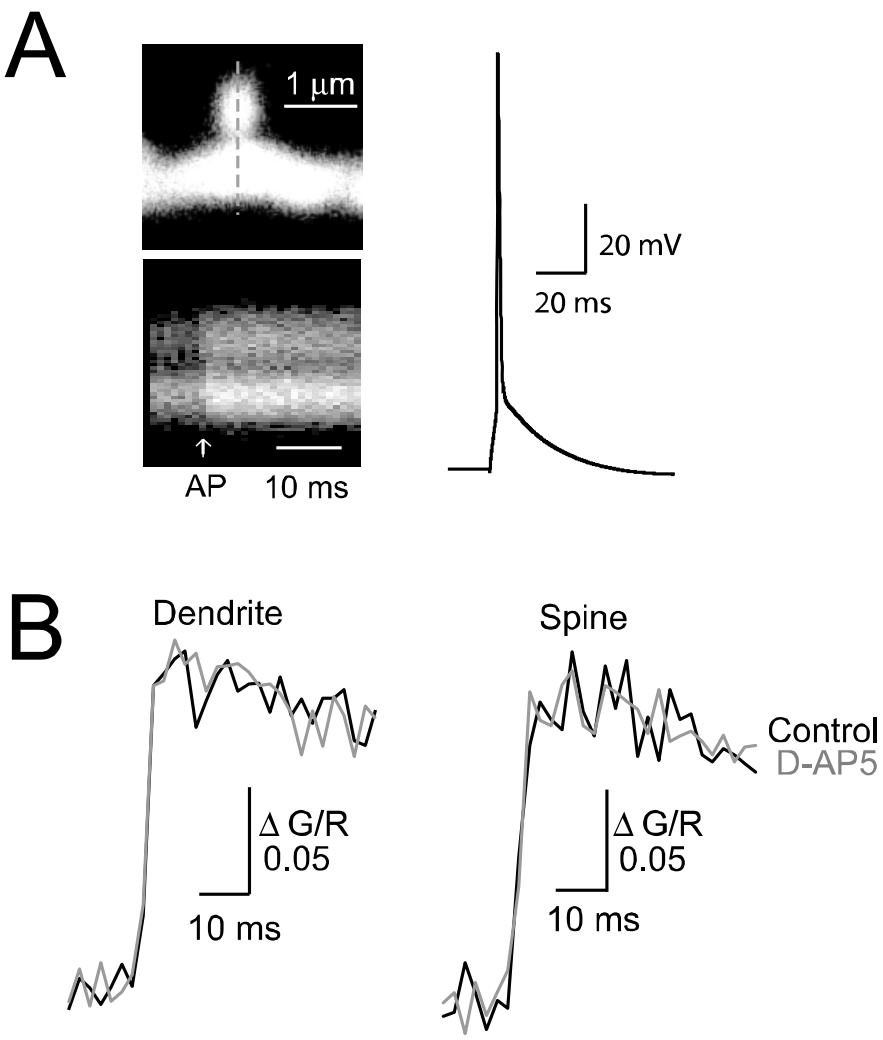

Figure 2. D-AP5 does not decrease the residual Ca^{2+} signal in dendrite or spine

(**A**) Average fluorescence transient collected in line-scan mode evoked by a 40 ms voltage step in dendrite (*left*) and spine (*right*). Voltage-gated Ca^{2+} channel signal was pharmacologically inhibited in all conditions. Line-scans were collected in control condition (black), 10 µM D-AP5 (red), after a 10 min D-AP5 washout (green), and in 5 µM NMDA (blue). (**B**) Histogram of the average fluorescence transient in each condition over many cells (n = 11). Significance was determined by Friedman ANOVA with Conover posthoc.

Figure 2.

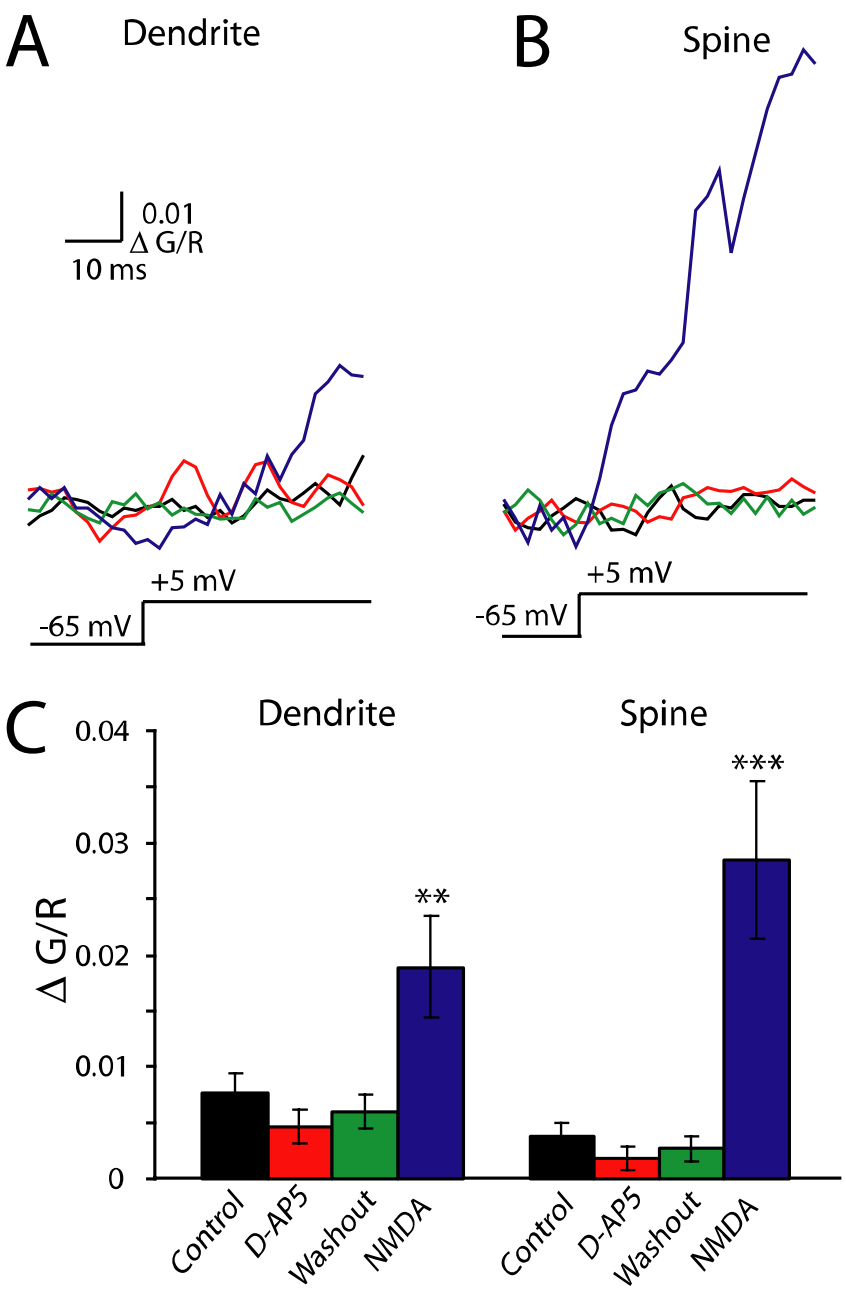
A
Dendrite
0.01
Δ G/R
10 ms
+5 mV
-65 mV
B
Spine
+5 mV
-65 mV
C
Dendrite
Spine
Δ G/R
0.04
0.03
0.02
0.01
0
**
***
Control
D-AP5
Washout
NMDA
Control
D-AP5
Washout
NMDA

Figure 3. Spine compartment is not preferentially protected by glutamate transporters

(**A1**) Average increase in fluorescence with a 40 ms mV voltage step in dendrite in response to control iontophoresis, L-aspartate ejection (black), ejection prevented with 2 nA backing current (red trace), release of backing current/ L-aspartate ejection recovery (gray trace), the addition of 100 µM TBOA (blue trace), and L-aspartate ejection prevented with backing current in the presence of TBOA (green).

(**A2**) Average response in each condition as normalized to 100 µM L-Aspartate without backing current (n = 5).

(**B1,2**) Same as in (**A1,2**) monitored simultaneously in spine.

Figure 3.

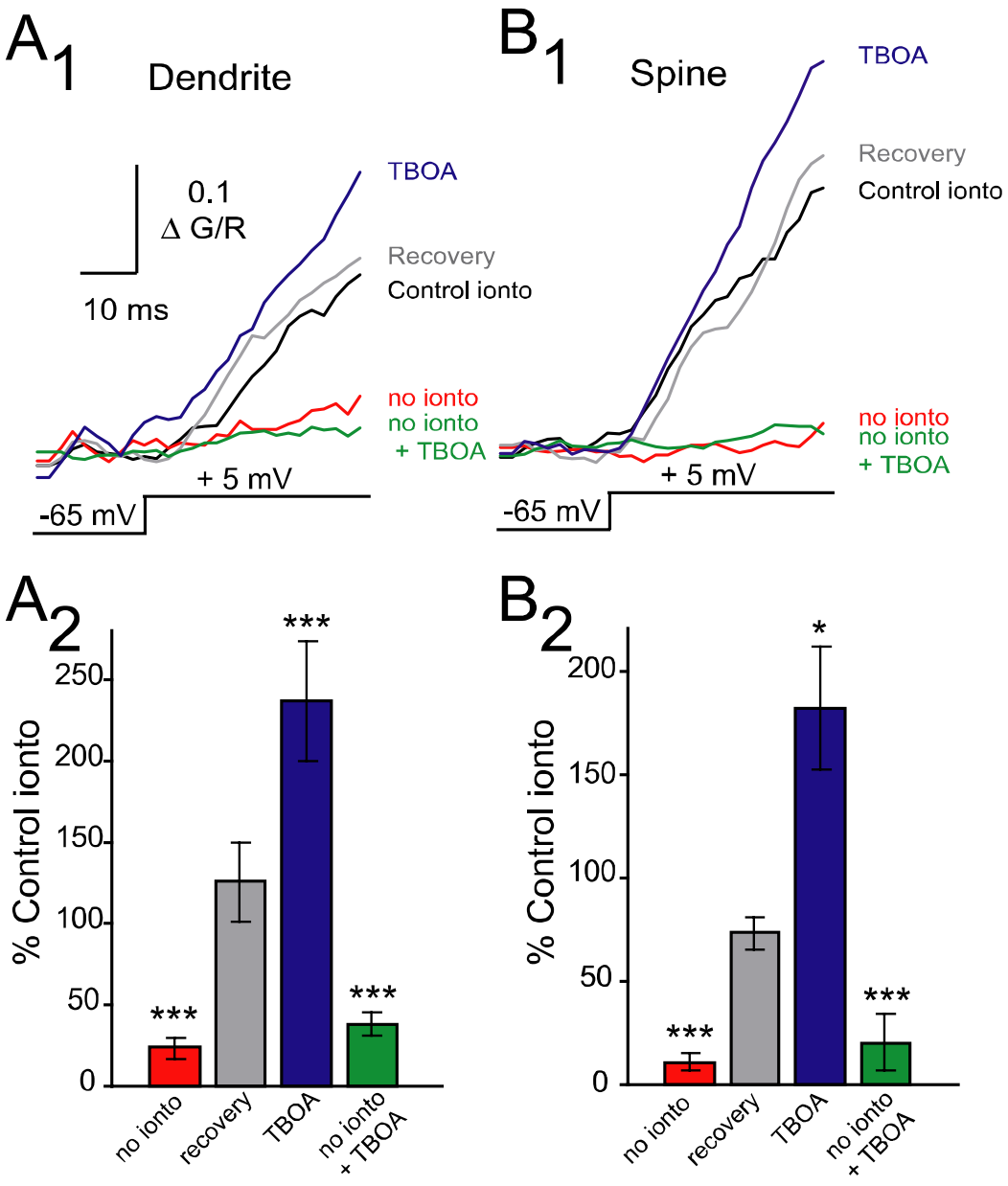
A1
Dendrite
0.1
Δ G/R
10 ms
TBOA
Recovery
Control ionto
no ionto
no ionto
+ TBOA
+ 5 mV
-65 mV
B1
Spine
TBOA
Recovery
Control ionto
no ionto
no ionto
+ TBOA
+ 5 mV
-65 mV
A2
% Control ionto
250
200
150
100
50
0
***
***
***
no ionto
recovery
TBOA
no ionto + TBOA
B2
% Control ionto
200
150
100
50
0
*
***
***
no ionto
recovery
TBOA
no ionto + TBOA

Discussion

In this dissertation, we show that transporters play a role in controlling glutamate concentrations on a range of time scales.

Transporters maintain a low concentration of ambient glutamate

The experiments described in Chapter 1 suggest that ambient glutamate in the extracellular space is ~25 nM. We addressed this issue because the strong driving force and high expression density of glutamate transporters in the extracellular space did not predict the range of ambient glutamate proposed by microdialysis experiments (1-4 μM). Our estimated concentration of 25 nM would cause negligible tonic activation of receptors, allowing them to function in the most sensitive capacity for detecting synaptic events.

The concentration of ambient glutamate that generates the standing NMDA receptor-mediated current is a balance between glutamate release and glutamate clearance by the transporters. Surprisingly, the source appears to be non-synaptic (Jaubadon et al., 1999; Cavelier and Attwell, 2005; Le Meur et al., 2007; Herman and Jahr, 2007), but its identity is still debated. Hypotheses for the identity of the source include the cysteine-glutamate exchanger (Baker et al., 2002), a non-specific anion channels on glial cells (Cavelier and Attwell, 2005), or the very slow diffusion of intracellular glutamate through the neuronal membrane bilayer to the extracellular space (Cavelier et al., 2005). However, inhibition of these sources has not decreased the baseline concentration of glutamate. Another potential source for ambient glutamate is the vesicular glutamate transporter (vGlut). The vGluts use a proton gradient to concentrate glutamate from the cytoplasm into the synaptic vesicle lumen (Edwards, 2007). After vesicle fusion, vGluts

may be positioned to extrude glutamate from the cytoplasm to the extracellular space driven by the glutamate concentration gradient, rather than relying on a proton gradient. This hypothesis is contingent on expression of vGluts on the plasma membrane, which has been suggested by Tarusawa et al. (2009) based on freeze fracture immuno-EM studies. The vGluts are intriguing as a potential source for ambient glutamate, and their role in this process warrants further investigation.

Future directions. To address the source of ambient glutamate, changes in the amplitude of the NMDA receptor-mediated standing current described in Chapter 1 would be examined. Experiment 1: Compare the NMDA receptor-mediated standing current revealed by flow pipe applied NMDA receptor antagonist in control and with vGluts blocked by the inhibitor Sky Blue. A decrease in the baseline standing current with Sky Blue would suggest a role for the vGluts as the ambient glutamate source. Experiment 2: Repeat experiment 1 in the presence of the transporter inhibitor, TBOA. Even if vGlut inhibitors cannot reduce the baseline standing current, it is possible that these molecules contribute to the increase in standing current when transporters are inhibited (Cavelier et al., 2005; Le Meur et al., 2007; Herman and Jahr, 2007). Experiment 3: Increase the number of vGluts on the plasma membrane by stimulating a barrage of activity using high potassium or hypertonic sucrose while blocking endocytosis with the dynamin inhibiting molecule dynasore (Newton et al., 2006; Hosoi et al., 2009). Compare the standing current in control conditions, post-stimulation, and post-stimulation in the presence of dynasore. If vGluts can extrude glutamate into the extracellular space when trapped on the surface, the high potassium or hypertonic sucrose treatment in the presence of dynasore should result in an increased NMDA receptor-

mediated standing current. Experiment 4: Dynasore has been shown to block endocytosis in cultured neurons and at the Calyx of Held (Newton et al., 2006; Hosoi et al., 2009), but not in hippocampal slice. Test the efficacy of dynasore by repeating the high release protocol (high potassium or hypertonic sucrose) in the presence of the styryl dye FM1-43 with and without dynasore. After washing away excess FM1-43, compare the number of stained vesicles between the dynasore and no dynasore conditions.

Ambient glutamate is low throughout the neuropil

Our estimate of the extracellular glutamate concentration, 25 nM, is much lower than previously reported by microdialysis (Lerma et al., 1986; Baker et al., 2002; Nyitrai et al., 2006). There are several possible explanations for this discrepancy. Some groups have suggested that the difference is due to the location of the sensors (i.e. the microdialysis probe versus NMDA receptors). This view proposes that ambient glutamate is compartmentalized in the extracellular space by physical barriers and by transporters that protect synaptic receptors (Pendyam et al., 2009). In this model, standing currents are generated only by the extrasynaptic NMDA receptors. In making the estimate of ambient glutamate, we normalized the standing current to a current generated by all the NMDA receptors on the cell by application of a non-transportable agonist. Because there are more synaptic than extrasynaptic NMDA receptors (Sobcyzk et al., 2005), the average standing current normalized to the whole cell NMDA-evoked current biases this estimate to the receptors sampling the synaptic extracellular compartment. Therefore, the ambient glutamate concentration as a function of receptor activation would appear very low. The microdialysis probe, on the other hand, indiscriminately samples all compartments in the extracellular space. This leads to the claim that the high microdialysis estimate reflects

the actual concentration of the extrasynaptic extracellular compartments in the neuropil (Pendyam et al., 2009; Kalivas, 2009). However, using two-photon microscopy, we tested this scenario in experiments described in Chapter 2 and found no difference between the tonic activation of synaptic and extrasynaptic NMDA receptors. Therefore, compartmentalization of glutamate into the non-synaptic extracellular space does not account for the discrepancy between our estimate and that made by microdialysis.

A more likely explanation for the nearly 100-fold difference in estimates with the two approaches is the amount of damage caused by the microdialysis probe. Though the microdialysis samples are not collected immediately following insertion (Xi et al., 2002; Baker et al., 2003), presumably to avoid contamination by glutamate released in response to the initial insult, the later samples collected after equilibration may be from chronically unhealthy tissue. An electron microscopy study suggests that there is a large volume of tissue damage surrounding the microdialysis probe insertion site, up to distances of 1.4 mm (Clapp-Lilly et al., 1999). It is unknown how the extracellular glutamate concentration is regulated in injured tissue, and it is possible that extensive damage could lead to glutamate build-up. Because the microdialysis probe is surrounded by damaged tissue, sampling the extracellular fluid from that region could lead to artificially high estimate of the ambient glutamate concentration.

Future directions. Our results from Chapters 1 and 2 are strong evidence that the ambient glutamate concentration is low in the extracellular space of hippocampal slice. However, a large body of work suggests a role for micromolar concentrations of ambient glutamate in the extracellular space of striatal nucleus accumbens (reviewed by Kalivas, 2009). Though we report in this thesis that the standing current generated by ambient glutamate

in the medium spiny neurons of striatal nucleus accumbens is equivalent to that produced in CA1 hippocampal neurons (Chapter 1; Supplemental Figure 1), this measurement is again a spatial and temporal average of all the NMDA receptors activated on the cell. The possibility remains that compartmentalization of ambient glutamate could occur in nucleus accumbens (Pendyam et al., 2009), even though it does not occur in hippocampus. Therefore, to test this, two-photon Ca^{2+} imaging experiments could be performed, as in Chapter 2, using medium spiny neurons. NMDA receptor-mediated Ca^{2+} signals have been observed in these neurons with synaptic stimulation and glutamate uncaging (Carter and Sabatini, 2004), suggesting that synapses, at least, contain these receptors. Comparing the tonic activation of NMDA receptors on the dendrite and spine of these neurons, using the localized Ca^{2+} signal and depolarization, will address whether compartmentalization of ambient glutamate occurs in brain regions other than hippocampus.

Conclusions

Glutamate transporters affect extracellular glutamate concentrations on time scales of minutes to milliseconds. By controlling these various glutamate concentrations, transporters preserve the precision of synaptic transmission. On the slowest time scale, transporters prevent buildup of ambient glutamate in the extracellular space. This role of transporters is crucial for preventing excitotoxic neuronal damage and maintaining a high sensitivity of receptors for detecting synaptic events. On a faster time scale, transporters limit spillover of synaptic glutamate, perhaps enhancing the level of synapse independence. This may be important for processing information in neuronal circuits and the whole brain. Additionally, on the fastest time scale, transporters control the time

course of the synaptic glutamate transient, which may limit the amount synaptic receptors are activated during a vesicle release event. Therefore, the roles of glutamate transporters range from preventing global neuronal cell damage to subtly altering the duration of synaptic events. Regardless of dynamic range of roles, without functional transporters glutamate concentrations would be unregulated, and the efficacy of synaptic transmission would be compromised.

References

Amara SG, Fontana ACK (2002) Excitatory amino acid transporters: keeping up with glutamate. Neurochem Intern 41:313-318.

Arnth-Jensen N, Jabaudon D, Scanziani M (2002) Cooperation between independent hippocampal synapses is controlled by glutamate uptake. Nat Neurosci 5:325-331.

Arriza JL, Eliasof S, Kavanaugh MP, Amara SG (1997) Excitatory amino acid transporter 5, a retinal glutamate transporter coupled to a chloride conductance. PNAS 94: 4155-4160.

Asztely F, Erdemli G, Kullmann DM (1997) Extrasynaptic glutamate spillover in the hippocampus; dependence on temperature and the role of active glutamate uptake. Neuron 18:281-293.

Atluri PP, Regehr WG (1996) Determinants of the time course of facilitation at the granule cell to Purkinje cell synapse. J Neurosci 16:5661-5671.

Atluri PP, Regehr WG (1998) Delayed release of neurotransmitter from cerebellar granule cells. J Neurosci 18:8214-8227.

Auger C, Attwell D (2000) Fast removal of synaptic glutamate by postsynaptic transporter. Neuron 28:547-558.

Baker DA, McFarland K, Lake RW, Shen H, Tang XC, Toda S, Kalivas PW (2003) Neuroadaptations in cystine-glutamate exchange underlie cocaine relapse. Nat Neurosci 6:743-749.

Baker DA, Xi ZX, Shen H, Swanson CJ, Kalivas PW (2002) The origin and neuronal function of *in vivo* nonsynaptic glutamate. J Neurosci 22:9134-9141.

Barbour B (2001) An evaluation of synapse independence. J Neurosci 21:7969-7984.

Barbour B, Keller BU, Llano I, Marty A (1994) Prolonged presence of glutamate during excitatory synaptic transmission to cerebellar Purkinje cells. Neuron 12:1331-1343.

Bergles DE, Jahr CE (1997) Synaptic activation of glutamate transporters in hippocampal astrocytes. Neuron 19:1297-1308.

Bergles DE, Tzingounis AV, Jahr CE (2002) Comparison of coupled and uncoupled currents during glutamate uptake by GLT-1 transporters. J Neurosci 22:10153-10162.

Blakely RD, Robinson MB, Amara SG (1988) Expression of neurotransmitter transport from rat brain mRNA in Xenopus laevis oocytes. Proc Natl Acad Sci U S A 85:9846-9850.

Blankenship AG, Ford KJ, Johnson J, Seal RP, Edwards RH, Copenhagen DR, Feller MB (2009) Synaptic and extrasynaptic factors governing glutamatergic retinal waves. Neuron 62:230-241.

Bloodgood BL, Sabatini BL (2007) Nonlinear regulation of unitary synaptic signals by CaV(2.3) voltage-sensitive calcium channels located in dendritic spines. Neuron 53:249-260.

Brasnjo G, Otis TS (2001) Neuronal glutamate transporters control activation of postsynaptic metabotropic glutamate receptors and influence cerebellar long-term depression. Neuron 31:607-616.

Brew H, Attwell D (1987) Electrogenic glutamate uptake is a major current carrier in the membrane of axolotl retinal glial cells. Nature 327:742.

Brickley SG, Revilla V, Cull-Candy SG, Wisden W, Farrant M (2001) Adaptive regulation of neuronal excitability by a voltage-independent potassium conductance. Nature 409:88-92

Bushong EA, Martone ME, Ellisman MH (2004) Maturation of astrocyte morphology and the establishment of astrocyte domains during postnatal hippocampal development. Int J Dev Neurosci 22:73-86.

Bushong EA, Martone ME, Jones YZ, Ellisman MH (2002) Protoplasmic astrocytes in CA1 stratum radiatum occupy separate anatomical domains. J Neurosci 22:183-192.

Carter AG, Sabatini BL (2004) State-dependent calcium signaling in dendritic spines of striatal medium spiny neurons. Neuron 44:483-493.

Carter AG, Regehr WG (2000) Prolonged synaptic currents and glutamate spillover at the parallel fiber to stellate cell synapse. J Neurosci 20:4423-4434.

Cavelier P, Attwell D (2005) Tonic release of glutamate by a DIDS-sensitive mechanism in rat hippocampal slices. J Physiol 564:397-410.

Cavelier P, Hamann M, Rossi D, Mobbs P, Attwell D (2005) Tonic excitation and inhibition of neurons: ambient transmitter sources and computational consequences. Prog Biophys Mol Biol 87:3-16.

Chaudhry FA, Lehre KP, van Lookeren Campagne M, Ottersen OP, Danbolt NC, Storm-Mathisen J (1995) Glutamate transporters in glial plasma membranes: highly differentiated localizations revealed by quantitative ultrastructural immunocytochemistry. Neuron 15:711-720.

Chiu CS, Jensen K, Sokolova I, Wang D, Li M, Deshpande P, Davidson N, Mody I, Quick MW, Quake SR, Lester HA (2002) Number, density, and surface/cytoplasmic distribution of GABA transporters at presynaptic structures of knock-in mice carrying GABA transporter subtype 1-green fluorescent protein fusions. J Neurosci 22:10251-10266.

Choi DW (1992) Excitotoxic cell death. J Neurobiol 23:1261-1276.

Choi S, Klingauf J, Tsien RW (2000) Postfusional regulation of cleft glutamate concentration during LTP at 'silent synapses'. Nat Neurosci 3:330-336.

Christie JM, Jahr CE (2008) Dendritic NMDA receptors activate axonal calcium channels. Neuron 60:298-307.

Christie JM, Jahr CE (2006) Multivesicular release at Schaffer collateral-CA1 hippocampal synapses. J Neurosci 26:210-216.

Clapp-Lilly KL, Roberts RC, Duffy LK, Irons KP, Hu Y, Drew KL (1999) An ultrastructural analysis of tissue surrounding a microdialysis probe. J Neurosci Methods 90:129-142.

Clark BA, Barbour B (1997) Currents evoked in Bergmann glial cells by parallel fibre stimulation in rat cerebellar slices. J Physiol 502:335-350.

Clements JD, Lester RA, Tong G, Jahr CE, Westbrook GL (1992) The time course of glutamate in the synaptic cleft. Science 258:1498-1501.

Conn PJ, Pin JP (1997) Pharmacology and functions of metabotropic glutamate receptors. Ann Rev Pharmacol Toxicol 37:205-237.

Danbolt NC (2001) Glutamate uptake. Prog Neurobiol 65:1-105.

Dehnes Y, Chaudhry FA, Ullensvang K, Lehre KP, Storm-Mathisen J, Danbolt NC

(1998) The glutamate transporter EAAT4 in rat cerebellar Purkinje cells: a glutamate-gated chloride channel concentrated near the synapse in parts of the dendritic membrane facing astroglia. J Neurosci 18:3606-3619.

Diamond JS (2005) Deriving the glutamate clearance time course from transporter currents in CA1 hippocampal astrocytes: transmitter uptake gets faster during development. J Neurosci 25:2906-2916.

Diamond JS (2002) A broad view of glutamate spillover. Nat Neurosci 5:291-292.

Diamond JS (2001) Neuronal glutamate transporters limit activation of NMDA receptors by neurotransmitter spillover on CA1 pyramidal cells. J. Neurosci. 21: 8328-8228.

Diamond JS, Bergles DE, Jahr CE (1998) Glutamate release monitored with astrocyte transporter currents during LTP. Neuron 21:425-433.

Diamond JS, Jahr CE (1995) Asynchronous release of synaptic vesicles determines the time course of the AMPA-receptor mediated EPSC. Neuron 15:1097-1107.

Diamond JS, Jahr CE (1997) Transporters buffer synaptically released glutamate on a submillisecond time scale. J Neurosci 17:4672-4687.

Diamond JS, Jahr CE (2000) Synaptically released glutamate does not overwhelm transporters on hippocampal astrocytes during high-frequency stimulation. J Neurophysiol 83:2835-2843.

Dowd LA, Coyle AJ, Rothstein JD, Pritchett DB, Robinson MB (1996) Comparison of Na^+-dependent glutamate transport activity in synaptosomes, C6 glioma, and Xenopus oocytes expressing excitatory amino acid carrier 1 (EAAC1). Mol Pharmacol 49:465-473

Dunwiddie TV, Diao L (1994) Extracellular adenosine concentrations in hippocampal brain slices and the tonic inhibitory modulation of evoked excitatory responses. J. Pharm Exp Ther 286:537-545.

Dzubay JA, Jahr CE (1999) The concentration of synaptically released glutamate outside of the climbing fiber-Purkinje cell synaptic cleft. J Neurosci 19:5265-5274.

Eccles JC, Jaeger JC (1958) The relationship between the mode of operation and the dimensions of junctional regions at synapses and motor end-organs. Proc R Soc Lond B Biol Sci 48:38-56.

Fairman WA, Vandenberg RJ, Arriza JL, Kavanaugh MP, Amara SG (1995) An excitatory amino-acid transporter with properties of a ligand-gated chloride channel. Nature 375: 599-603.

Featherstone DE, Shippy SA (2008) Regulation of synaptic transmission by ambient extracellular glutamate. Neuroscientist 14:171-181.

Fiacco TA, Agulhon C, Taves SR, Petravicz J, Casper KB, Dong X, Chen J, McCarthy KD (2007) Selective stimulation of astrocyte calcium in situ does not affect neuronal excitatory synaptic activity. Neuron 54:611-626.

Foster KA, Crowley JJ, Regehr WG (2005) The influence of multivesicular release and postsynaptic receptor saturation on transmission at granule cell to Purkinje cell synapses. J Neurosci 25:11655-11665.

Franks KM, Bartol TM Jr, Sejnowski TJ (2002) A Monte Carlo model reveals independent signaling at central glutamatergic synapses. Biophys J 83:2333-2348.

Fritschy JM (2008) Is my antibody-staining specific? How to deal with pitfalls of immunohistochemistry. Eur J Neurosci 28:2365-2370.

Furness DN, Dehnes Y, Akhtar AQ, Rossi DJ, Hamann M, Grutle NJ, Gundersen V, Holmseth S, Lehre KP, Ullensvang K, Wojewodzic M, Zhou Y, Attwell D, Danbolt NC (2008) A quantitative assessment of glutamate uptake into hippocampal synaptic terminals and astrocytes: new insights into a neuronal role for excitatory amino acid transporter 2 (EAAT2). Neuroscience 157:80-94.

Garthwaite J (1985) Cellular uptake disguises action of L-glutamate on N-methyl-D-aspartate receptors. With an appendix: diffusion of amino acids into brain slices. Br J Pharmacol 85:297-307.

Goda Y, Stevens CF (1994) Two components of transmitter release at a central synapse. Proc Natl Acad Sci USA 91:12942-12946.

Haber M, Zhou L, Murai KK (2006) Cooperative astrocyte and dendritic spine dynamics at hippocampal excitatory synapses. J Neurosci 26:8881-8891.

Harrison J, Jahr CE (2003) Receptor occupancy limits synaptic depression at climbing fiber synapses. J Neurosci 23:377-383.

Herman MA, Jahr CE (2007) Extracellular glutamate concentration in hippocampal slice. J Neurosci 27:9736-9741

Hestrin S, Sah P, Nicoll RA (1990) Mechanisms generating the time course of dual component excitatory synaptic currents recorded in hippocampal slices. Neuron 5:247-253.

Hertz L (1979) Functional interactions between neurons and astrocytes I. Turnover and metabolism of putative amino acid transmitters. Prog Neurobiol 13:277-323.

Higley MJ, Soler-Llavina GJ, Sabatini BL (2009) Cholinergic modulation of multivesicular release regulates striatal synaptic potency and integration. Nat Neurosci 12:1121-1128.

Hille B (1984) Ionic channels of excitable membranes, Ed 1. Sunderland, MA: Sinauer Associates.

Hires SA, Zhu Y, Tsien RY (2008) Optical measurement of synaptic glutamate spillover and reuptake by linker optimized glutamate-sensitive fluorescent reporters. Proc Natl Acad Sci USA 105:4411-4416.

Hosoi N, Holt M, Sakaba T (2009) Calcium dependence of exo- and endocytosis coupling at a glutamatergic synapse. Neuron 63:216-229.

Isaacson JS, Nicoll RA (1993) The uptake inhibitor L-*trans*-PDC enhances responses to glutamate but fails to alter the kinetics of excitatory synaptic currents in the hippocampus. J Neurophysiol 70:2187-2191.

Jabaudon D, Shimamoto K, Yasuda-Kamatani Y, Scanziani M, Gähwiler BH, Gerber U (1999) Inhibition of uptake unmasks rapid extracellular turnover of glutamate of nonvesicular origin. Proc Natl Acad Sci USA 96:8733-8738.

Kalivas PW (2009) The glutamate homeostasis hypothesis of addiction. Nat Rev Neurosci 10:561-572.

Kampa BM, Clements J, Jonas P, Stuart GJ (2004) Kinetics of Mg^{2+} unblock of NMDA receptors: implications for spike-timing dependent plasticity. J Physiol 556:337-345

Kanai Y, Hediger MA (1992) Primary structure and functional characterization of high-affinity glutamate transporter. Nature 360: 467-471.

Kanai Y, Nussberger S, Romero MF, Boron WF, Herbert SC, Hediger MA (1995) Electrogenic properties of the epithelial and neuronal high affinity glutamate transporter. J Biol Chem 270:16561-16568.

Kanner B (2006) Structure and function of sodium-coupled GABA and glutamate transporters. J Membr Biol 213:89-100.

Katz B, Miledi R (1973) The binding of acetylcholine to receptors and its removal form the synaptic cleft. J Physiol 231:549-574.

Kavanaugh MP, Arriza JL, North RA, Amara SG (1992) Electrogenic uptake of gamma-aminobutyric acid by cloned transporters in Xenopus oocytes. J Biol Chem 267:22007-22009.

Lauri SE, Vesikansa A, Segerstrale M, Collinridge GL, Isaac JT, Taira T (2006) Functional maturation of CA1 synapses involves activity-dependent loss of tonic kainate receptor-mediated inhibition of glutamate release. Neuron 50:415-429.

Le Meur K, Galante M, Angulo MC, Audinat E (2007) Tonic activation of NMDA receptors by ambient glutamate of non-synaptic origin in the rat hippocampus. J Physiol 580:373-383.

Lehre KP, Danbolt NC (1998) The number of glutamate transporter subtype molecules at glutamatergic synapses: chemical and stereological quantification in young adult rat brain. J Neurosci 18:8751-8757.

Lehre KP, Levy LM, Ottersen OP, Storm-Mathisen J, Danbolt NC (1995) Differential expression of two glial glutamate transporters in the rat brain: quantitative and immunocytochemical observations. J Neurosci 15: 1835-1853.

Lehre KP, Rusakov DA (2002) Asymmetry of glia near central synapses favors

presynaptically directed glutamate escape. Biophys J 83:125-134.

Lerma J, Herranz, AS, Herreras O, Abraira V, Martin Del Rio R (1986) *In vivo* determination of extracellular concentration of amino acids in the rat hippocampus. A method based on brain dialysis and computerized analysis. Brain Res 384:145-155.

Lester RAJ, Jahr CE (1992) NMDA channel behavior depends on agonist affinity. J Neurosci 12:635-643.

Levy LM, Attwell D, Hoover F, Ash JF, Bjoras M, Danbolt NC (1998) Inducible expression of the GLT-1 glutamate transporter in a CHO cell line selected for low endogenous glutamate uptake. FEBS Lett 422:339–342.

Linden DJ (1997) Long-term potentiation of glial synaptic currents in cerebellar culture. Neuron 18:983-994.

Loo DD, Eskandari S, Boorer KJ, Sarkar HK, Wright EM (2000) Role of Cl- in electrogenic Na^+-coupled cotransporters GAT1 and SGLT1. J Biol Chem 275:37414-37422.

Mainen ZF, Malinow R, Svoboda K (1999) Synaptic calcium transients in single spines indicate that NMDA receptors are not saturated. Nature 399:427-430.

Matsuzaki M, Honkura N, Ellis-Davies GC, Kasai H (2004) Structural basis of long-term potentiation in single dendritic spines. Nature 429:761-766.

McAllister AK, Stevens CF (2000) Nonsaturation of AMPA and NMDA receptors at hippocampal synapses. Proc Natl Acad Sci U S A 97:6173-6178.

McFarland K, Lapish CC, Kalivas PW (2003) Prefrontal glutamate release into the core of the nucleus accumbens mediates cocaine-induced reinstatement of drug-seeking behavior. J Neurosci 23: 3531-3537.

Mennerick S, Zorumski CF (1994) Glial contributions to excitatory neurotransmission in cultured hippocampal cells. Nature 368:59-62.

Min MY, Rusakov DA, Kullmann DM (1998) Activation of AMPA, kainate, and metabotropic receptors at hippocampal mossy fiber synapses: role of glutamate diffusion. Neuron 21:561-570.

Moran MM, McFarland K, Melendez RI, Kalivas PW, Seamans JK (2005) Cystine/glutamate exchange regulates metabotropic glutamate receptor presynaptic inhibition of excitatory transmission and vulnerability to cocaine seeking. J Neurosci 25:6389-6393.

Newton AJ, Kirchhausen T, Murthy VN (2006) Inhibition of dynamin completely blocks compensatory synaptic vesicle endocytosis. Proc Natl Acad Sci U S A 103: 17955-17960.

Nie H, Weng HR (2009) Glutamate transporters prevent excessive activation of NMDA receptors and extrasynaptic glutamate spillover in the spinal dorsal horn. J Neurophysiol 101:2041-2051.

Nielsen TA, DiGregorio DA, Silver RA (2004) Modulation of glutamate mobility reveals the mechanism underlying slow-rising AMPAR EPSCs and the diffusion coefficient in the synaptic cleft. Neuron 42:757-771.

Nimchinsky EA, Yasuda R, Oertner TG, Svoboda K (2004) The number of glutamate receptors opened by synaptic stimulation in single hippocampal spines. J Neurosci 24:2054-2064.

Nyitrai G, Kékesi KA, Juhász G (2006) Extracellular level of GABA and Glu: *In vivo* microdialysis-HPLC measurements. Curr Top Med Chem 6:935-940.

Oertner TG, Sabatini BL, Nimchinsky EA, Svoboda K (2002) Facilitation at single synapses probed with optical quantal analysis. Nat Neurosci 5:657-664.

Otis TS, Kavanaugh MP, Jahr CE (2001) Postsynaptic glutamate transport at the parallel fiber-Purkinje cell synapse. Science 277:1515-1518.

Palay SL, and Chan-Palay V. (1974) Cerebellar Cortex: Cytology and Organization. New York, Springer-Verlag.Patneau DK, Mayer ML (1990) Structure-activity relationships for amino acid transmitter candidates acting at *N*-methyl-D-aspartate and quisqualate receptors. J Neurosci 10:2385-2399.

Patneau DK, Mayer ML (1990) Structure-activity relationships for amino acid transmitter candidates acting at *N*-methyl-D-aspartate and quisqualate receptors. J Neurosci 10:2385-2399.

Pendyam S, Mohan A, Kalivas P, Nair SS (2009) Computational model of extracellular glutamate in the nucleus accumbens incorporates neuroadaptations by chronic cocaine. Neuroscience 158:1266-1276.

Pierce RC, Bell K, Duffy P, Kalivas PW (1996) Repeated cocaine augments excitatory amino acid transmission in the nucleus accumbens only in rats having developed behavioral sensitization. J Neurosci 16:1550-1560.

Pines G, Danbolt NC, Bjoras M, Zhang Y, Bednahan A, Eide L, Koepsell H, Storm-Mathisen J, Seeberg E, Kanner BI (1992) Cloning and expression of a rat brain L-glutamate transporter. Nature 360: 464-467.

Pologruto TA, Sabitini BL, Svoboda K (2003) ScanImage: flexible software for operating laser scanning microscopes. Biomed Eng Online 2:13.

Postlethwaite M, Hennig MH, Steinert JR, Graham BP, Forsythe ID (2007) Acceleration of AMPA receptor kinetics underlies temperature-dependent changes in synaptic strength at the rat calyx of Held. J Physiol 579:69-84.

Priestley T, Laughton P, Myers J, Le Bourdelles B, Kerby J, Whiting PJ (1995) Pharmacological properties of recombinant human N-methyl-D-aspartate receptors comprising NR1a/NR2A and NR1a/NR2B subunit assemblies expressed in permanently transfected mouse fibroblast cell. Mol Pharmolocl 48:841-848.

Rossi DJ, Oshima T, Attwell D (2000) Glutamate release in severe brain ischaemia is mainly by reversed uptake. Nature 403:316-321.

Rossi DJ, Slater NT (1993) The developmental onset of NMDA receptor-channel activity during neuronal migration. Neuropsychopharm. 32:1239-1248.

Rothstein JD, Dykes-Hoberg M, Pardo CA, Briston LA, Jin L, Kunci RW, Kanai Y, Hediger MA, Wang Y, Scheilke JP, Welty DF (1996) Knockout of glutamate transporters reveals a major role for astroglial transport in excitotoxicity and clearance of glutamate. Neuron 16:675-686.

Rothstein JD, Martin L, Levey AI, Dykes-Hoberg M, Jin L, Wu D, Nash N, Kuncl RW (1994) Localization of neuronal and glial glutamate transporters. Neuron 13:713-725.

Rusakov DA, Kullmann DM (1998) Extrasynaptic glutamate diffusion in the hippocampus: ultrastructural constraints, uptake, and receptor activation. J Neurosci 18:3158-3170.

Sabatini BL, Oertner TG, Svoboda K (2002) The life cycle of Ca^{2+} ions in dendritic spines. Neuron33:439-452.

Sah P, Hestrin S, Nicoll RA (1989) Tonic activation of NMDA receptors by ambient glutamate enhances excitability of neurons. Science 246:815-818.

Santhakumar V, Hanchar HJ, Wallner M, Olsen RW, Otis TS (2006) Contributions of GABAA receptor alpha6 subunit to phasic and tonic inhibition revealed by a naturally occurring polymorphism in the alpha6 gene. J Neurosci 26:3357-3364.

Santhakumar V, Wallner M, Otis TS (2007) Ethanol acts directly on extrasynaptic subtypes of GABAA receptors to increase tonic inhibition. Alcohol 41:211-221.

Sarantis M, Ballerini L, Miller B, Silver RA, Edwards M, Atwell D (1993) Glutamate uptake from the synaptic cleft does not shape the decay of the non-NMDA component of the synaptic current. Neuron 11:541-549.

Savtchenko LP, Rusakov DA (2007) The optimal height of the synaptic cleft. Proc Natl Acad Sci U S A 104:1823-1828.

Scanziani M, Salin PA, Vogt KE, Malenka RC, Nicoll RA (1997) Use-dependent increases in glutamate concentration activate presynaptic metabotropic glutamate receptors. Nature 385:630-634.

Sobczyk A, Scheuss V, Svoboda K (2005) NMDA receptor subunit-dependent [Ca^{2+}] signaling in individual hippocampal dendritic spines. J Neurosci 25:6037-6046.

Spacek J (1985) Three-dimensional analysis of dendritic spines. III. Glial Sheath. Anat

Embryol (Berl) 171:245-252

Szapiro G, Barbour B (2007) Multiple climbing fibers signal to molecular layer interneurons exclusively via glutamate spillover. Nat Neurosci 10:735-742.

Storck T, Schulte S, Hofmann K, Stoffel W (1992) Structure, expression, and functional analysis of a Na^+-dependent glutamate/ aspartate transporter from rat brain. PNAS 89:10955-10959

Takahashi M, Sarantis M, Attwell D (1996) Postsynaptic glutamate uptake in rat cerebellar Purkinje cells. J Physiol 497:523-530.

Takahashi T, Kovalchu K, Atwell D (1995) Pre- and postsynaptic determinants of EPSC waveform at cerebellar climbing fiber and parallel fiber to Purkinje cell synapses. J Neurosci 15:5693-5702.

Takayasu Y, Iino M, Shimamoto K, Tanaka K, Ozawa S (2006) Glial glutamate transporters maintain a one-to-one relationship at the climbing fiber-Purkinje cell synapse by preventing glutamate spillover. J Neurosci 26:6563-6572.

Tanaka K, Watase K, Manabe T, Yamada K, Watanabe M, Takahashi K, Iwama H, Nishikawa T, Ichihara N, Kikuchi T, Okuyama S, Kawashima N, Hori S, Takimoto M, Wada K (1997) Epilepsy and exacerbation of brain injury in mice lacking the glutamate transporter Glt-1. Science 276:1699-1702.

Tarusawa E, Matsui K, Budisantoso T, Molnár E, Watanabe M, Matsui M, Fukazawa Y, Shigemoto R (2009) Input-specific intrasynaptic arrangements of ionotropic glutamate receptors and their impact on postsynaptic responses. J Neurosci 29:12896-12908.

Tong G, Jahr CE (1994) Block of glutamate transporters potentiates postsynaptic excitation. Neuron 13:1195-1203.Trussell LO, Fischbach GD (1989) Glutamate receptor desensitization and its role in synaptic transmission. Neuron 3:209-218.

Trussell LO, Fischbach GD (1989) Glutamate receptor desensitization and its role in synaptic transmission. Neuron 3:209-218.

Tzingounis AV, Wadiche JI (2007) Glutamate transporters: confining runaway excitation by shaping synaptic transmission. Nat Rev Neurosci 8:935-947.

Ventura R, Harris KM (1999) Three-dimensional relationships between hippocampal synapses and astrocytes. J Neurosci 19:6897-6906.

Vizi ES (2000) Role of high-affinity receptors and membrane transporters in nonsynaptic communication and drug action in the central nervous system. Pharmacol Rev 52:63-89.

Wadiche JI, Amara SG, Kavanaugh MP (1995a) Ion fluxes associated with excitatory amino acid transport. Neuron 15: 721-728

Wadiche JI, Arriza JL, Amara SG, Kavanaugh MP (1995b) Kinetics of a human glutamate transporter. Neuron 14:1019-1027.

Wadiche JI, Jahr CE (2001) Multivesicular release at climbing fiber-Purkinje cell synapses. Neuron 25:301-313.

Wadiche JI, Jahr CE (2005) Patterned expression of Purkinje cell glutamate transporters controls synaptic plasticity. Nat Neurosci 8:1329-1334.

Wadiche JI, Kavanaugh MP (1998) Macroscopic and microscopic properties of a cloned glutamate transporter/chloride channel. J Neurosci 18:7650-7661.

Wadiche JI, Tzingounis AV, Jahr CE (2006) Intrinsic kinetics determine the time course of neuronal synaptic transporter currents. Proc Natl Acad Sci USA 103:1083-1087.

Watanabe J, Rozov A, Wollmuth LP (2005) Target-specific regulation of synaptic amplitudes in the neocortex. J Neurosci 25:1024-1033.

Westergren L, Nystrom B, Hamberger A, Johansson BB (1995) Intracerebral dialysis and the blood brain barrier. J Neurochem 64:229–234.

Witcher MR, Kirov SA, Harris KM (2007) Plasticity of perisynaptic astroglia during synaptogenesis in the mature rat hippocampus. Glia 55:13-23.

Xi ZX, Baker DA, Shen H, Carson DS, Kalivas PW (2002) Group II metabotropic glutamate receptors modulate extracellular glutamate in the nucleus accumbens. J Pharmacol Exp Ther 300:162-171.

Xu-Friedman MA, Harris KM, Regehr WG (2001) Three-dimensional comparison of ultrastructural characteristics at depressing and facilitating synapses onto cerebellar Purkinje cells. J Neurosci 6666-6672.

Yamashita T, Kanda T, Equchi K, Takahashi T (2009) Vesicular glutamate filling and AMPA receptor occupancy at the calyx of Held synapse of immature rats. J Physiol 587:2327-2339

Zacks SI, Blumberg JM (1961) The histochemical localization of acetycholinesterase in the fine structure of neuromuscular junctions of mouse and human intercostal muscle. J Histochem Cytochem 9:317-325.

Zerangue N, Kavanaugh M (1996) Flux coupling in a neuronal glutamate transporter. Nature 383:634-637.

Zheng K, Scimemi A, Rusakov D (2008) Receptor actions of synaptically released glutamate: the role of transporters on the scale from nanometers to microns. Biophys J 95:4584-4596.

Zhou J, Sutherland ML (2004) Glutamate transporter cluster formation in astrocytic processes regulates glutamate uptake activity. J Neurosci 24:6301-6306.